ANNUAL REPORT

FOR

SOLAR CELL RESEARCH

Prepared Under:

WORK ORDER 8056

Prepared By:

R. L. Statler
N. D. Wilsey
J. E. Stannard
J. Comas
B. J. Faraday

Naval Research Laboratory
Solid State Applications Branch
Washington, D. C. 20390

15 October 1969

ANNUAL REPORT

FOR

SOLAR CELL RESEARCH

Work Done By:

C. A. Carosella
J. Comas
B. J. Faraday
R. J. Lambert
J. E. Stannard
R. L. Statler
N. D. Wilsey

Report Written By:

R. L. Statler
N. D. Wilsey
J. E. Stannard
J. Comas
B. J. Faraday

Prepared By:

Naval Research Laboratory
Solid State Applications Branch
Washington, D. C. 20390

Under Work Order 8056

This work was performed for the Jet Propulsion Laboratory, California Institute of Technology, as sponsored by the National Aeronautics and Space Administration under Contract NAS 7-100.

This report contains information prepared by the Naval Research Laboratory under JPL sub-contract. Its content is not necessarily endorsed by the Jet Propulsion Laboratory, California Institute of Technology, or by the National Aeronautics and Space Administration.

R. L. Statler
Program Manager

E. L. Brancato
Program Supervisor

ABSTRACT

This report covers twelve months of progress on solar cell research.

(1) Room temperature annealing in 1 MeV electron damaged lithium-diffused silicon was studied using the Hall effect between 10°K and 300°K. The results indicate that low temperature irradiation is required for separation of the damage and annealing processes. A radiation induced deep center was observed at 0.15 eV below the conduction band.

(2) A study of low flux Co^{60} gamma irradiation of lithium-diffused silicon solar cells revealed the presence of a continuing damage stage in the cell parameters after exposure up to 4.2×10^{15} 1 MeV e/cm^2 equivalent absorbed dose.

(3) Successful ion implantation techniques were developed and demonstrated by boron implantation in a silicon diode using a focused controlled ion beam.

(4) Preliminary measurements of 10 ohm-cm n/p solar cells irradiated with 1 MeV electrons at 115°K showed an increased rate of damage compared with 300°K irradiation.

(5) A computer program was written to obtain the diode parameters of a solar cell by a least-squares fitting of I-V data to the solar cell equation. Quite good fits to data were made by this process using four adjustable parameters.

(6) Chapters II, III, and IV of the Handbook on Space Environmental Effects on Solar Cell Power Systems were reviewed. A new format is recommended, based on results of interviewing many solar cell users.

CONTENTS

ILLUSTRATIONS

TABLES

1.0 INTRODUCTION

This is the final report on National Aeronautics and Space Administration DPR WO-8056 for the Jet Propulsion Laboratory, California Institute of Technology. The period of work performed extended from October 15, 1968 to October 15, 1969.

The major portion of the research program comprises a number of study areas which are directed toward understanding and improving the radiation resistance of silicon solar cells. These areas of study include investigating radiation effects in silicon crystals (e.g. the behavior of lithium in silicon), studying problems relating to the formation of electrical contacts to solar cells, and the measurement and evaluation of properties of manufactured solar cells.

The objective of the bulk silicon study is to develop a better understanding of the radiation damage model for lithium-diffused solar cells. The approach to this task is to utilize the measurement of Hall coefficient in irradiated lithium diffused silicon as a function of temperature, fluence, and post-irradiation thermal annealing time. The unique feature of the Hall measurement as a function of temperature between $4^{\circ}K$ and $300^{\circ}K$ is that a separate determination of acceptor and donor concentrations can be made in materials where one type of each is present. During the contract period, this technique was utilized to identify the energy levels and annealing kinetics of donor and acceptor states in float-zone silicon doped with lithium.

Another aspect of the effect of lithium in irradiated silicon is being investigated. In this experiment the photovoltaic properties of lithium-diffused solar cells are evaluated as a function of temperature of irradiation at low flux rates. During the first part of the contract period, this work was a continuation of an experiment initiated in June 1967 at NASA-GSFC. After several months this experiment was terminated and the experience gained resulted in the design of an improved experiment. Sixty-five cells are now being irradiated by low fluence Co^{60} gamma rays at two temperatures.

During the recent past, solar cell contact problems have been recognized as one cause of space power system degradation. One portion of the present contract relevant to this situation is concerned with making improved solar cell contacts by using ion implantation and sputtering techniques. The apparatus for producing ion beams with energy up to 30 KeV was constructed and successfully used to implant boron into a Schottky

diode, thereby altering its electrical properties. A metallic ion source was purchased for use on the 30 KeV accelerator for the purpose of implanting metallic contacts on semiconductor surfaces.

Another phase of the program for evaluating solar cell properties is concerned with the effect of radiation on silicon solar cells at low temperatures. In conjunction with low temperature irradiations, the photovoltaic properties are also measured at low temperatures as a function of intensity of illumination. The knowledge gained from this work will be applicable to calculating power system requirements for outer planetary satellite missions. This requires cell temperatures at least as low as $125^{o}K$ and illumination intensities as small as $5mW/cm^2$.

The study of solar cell characteristics is being carried out by detailed analysis of the I-V curve using a computer program. Through a curve fitting process using the diode equation and photovoltaic current-voltage data, the best-fit values for R_s, I_o, A, and I_L can be obtained. The computer program has been written for the four adjustable-parameter equation. The curve-fitting has been quite good.

Finally one task in the contract is to review the Handbook of Space Environmental Effects on Solar Cell Power Systems for applicability by power systems engineers. Chapters II, III, and IV have been reviewed in specific detail. The general format for a new edition of a handbook is suggested as a result of personal interviews with many members of the solar cell community.

2.0 DISCUSSION

2.1 Radiation Effects in Lithium-Diffused Silicon

2.1.1. Introduction. At the present time there is no detailed model for the interaction of lithium with any of the several known radiation damage centers [1] in n-type silicon. Equally unknown is the effect such interactions have upon the minority carrier capture cross-sections of these centers.

Work performed under this contract has been restricted to Hall and resistivity measurements as a function of temperature in bulk n-type silicon doped with lithium by diffusion. Such measurements allow defect concentrations to be determined but do not give evidence as to the effects these defects may have upon minority carrier lifetime. This study represents the first application of transport measurements at liquid helium temperatures to the study of electron damage in Si(Li).

The Hall effect has been used extensively to measure impurity and damage center concentrations in semiconductors.[2-4] In fact it is still the most sensitive tool available for such determinations. When performed as a function of temperature between 4°K and 300°K on a semiconductor containing one type of acceptor and one type of donor, the measurement allows a separate determination of these two concentrations. In addition the location of one of the levels in the forbidden gap may be determined. Hall effect studies of radiation damage in lithium-doped silicon until now have been limited to temperatures above 77°K.[2,4] Such a measurement allows a quantity equal to the donor concentration minus the acceptor concentration to be determined. This means the creation of an acceptor affects the measured quantity in the same way as the loss of a donor. Both of these processes are presumed to occur for radiation damage in Si(Li) and cannot be separated in a measurement restricted to high temperatures.

2.1.2. Hall Effect. Before discussing experimental results, some comments on the Hall effect at low temperatures and in particular the application of this tool to damaged material is in order. Hall effect allows the carrier concentration to be measured to within a proportionality factor known as the Hall factor. The Hall factor is a function of temperature and magnetic field. Its numerical value ranges from 0.9 to 2.0 in magnitude.[5-7] In our experiments all measurements were made with magnetic fields in the low field limit ($B<500$ Oe), where the Hall factor is independent of magnetic field. Further corrections for this factor depend upon the properties of the individual samples and will be considered later.

If the defects present in a semiconductor are known, the carrier concentration can be calculated as a function of temperature. This is done by requiring that local charge neutrality be satisfied and that Fermi statistics govern the electron occupation of defect states. In this work however, the carrier concentration is known and the defects are to be calculated. In general, this reverse calculation need not lead to a unique set of defect states. In the case of a semiconductor containing only one kind of donor and one kind of acceptor this reverse calculation is relatively straight forward. A two impurity system, as treated in Appendix A, contains four parameters which are adjusted to fit the data. The four parameters used are donor and acceptor concentrations, donor degeneracy factor, and low temperature Fermi level. Values of the parameters obtained in this way can identify a defect through a characteristic value of the low temperature Fermi energy and can indicate the concentration of that defect. The analysis of data obtained in a more complicated system requires some caution.

The material studied here was found to contain three types of shallow impurity donors, (Li^+, LiO^+, P^+). In addition it presumably contained shallow impurity acceptors and several kinds of deep acceptors due to radiation damage. Attempts were made to fit the data from this sample to a number of models. These included two and three impurity models, and two impurity models with donor excited states. The two impurity model reported here gave the best fits.

Figure 1 shows the defect states representative of electron damaged Si(Li). The electron occupations shown are characteristic of low temperatures, and are reasonably accurate up to $40^{\circ}K$. All states above the low temperature Fermi level may be considered empty and all those below filled. The Fermi level is that position in the forbidden gap where the probability for a level to be filled is 1/2. In general the low temperature Fermi level is pinned at the defect which is partly occupied. Exactly which defect level pins the Fermi level will depend on the balance between donor states above this defect level and acceptor states below.

These concepts are useful in showing that even in material as complicated as electron damaged Si(Li) the two impurity model can be used to obtain knowledge about defect states from the carrier concentration. The amount of information depends upon the location of the low temperature Fermi level.

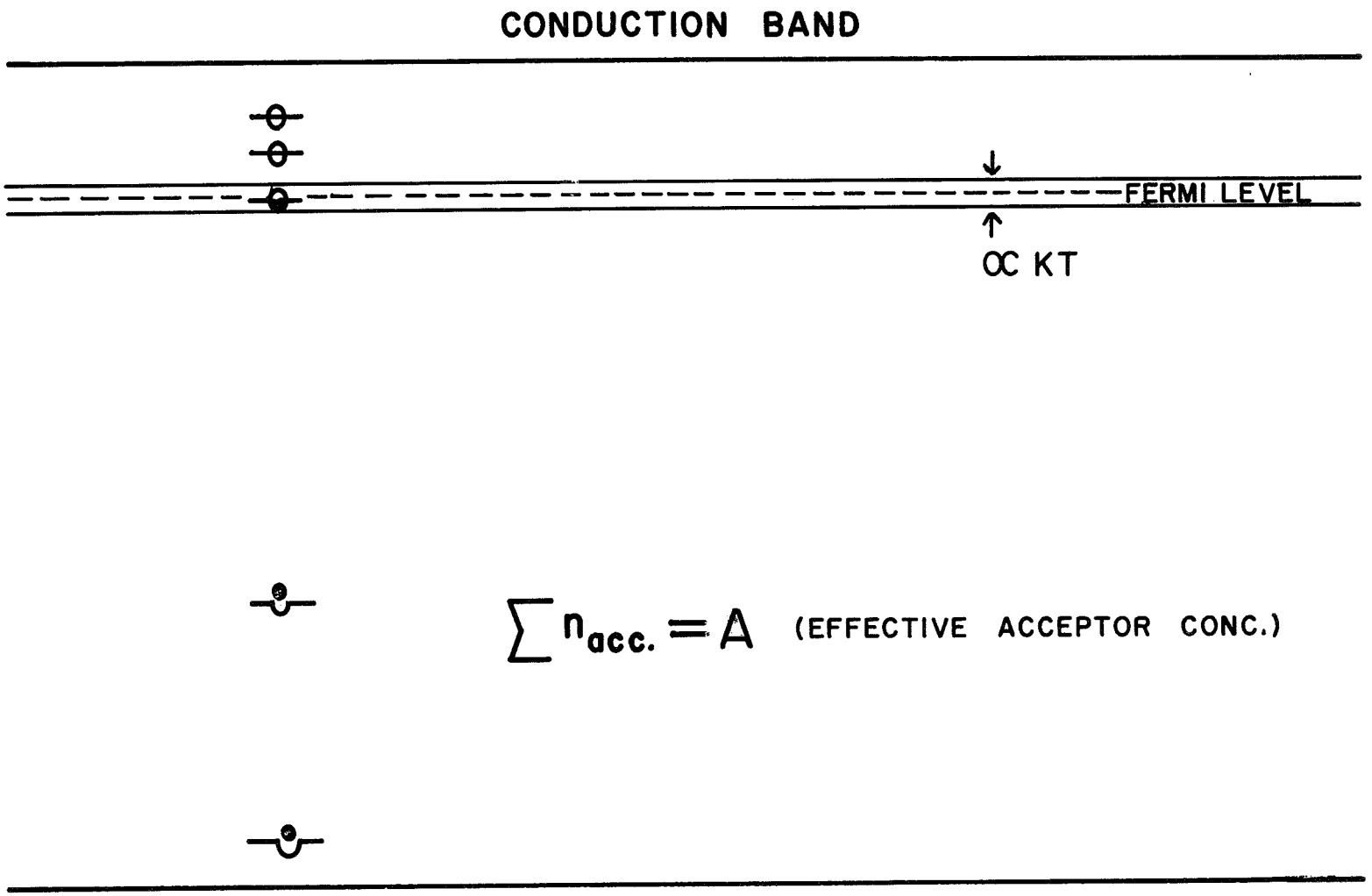

Figure 1 The two impurity model at low temperature for electron irradiated Si(Li). All levels below the Fermi level are occupied by electrons, and all those above are unoccupied.

Case I:

Presume that the low temperature Fermi level coincides with the level of the shallowest donor present. In this material this is the free lithium donor level.

The acceptors in the lower half of the gap are filled at all temperatures so their presence can be approximated by a single acceptor level of concentration A. The donors near the conduction band are assumed to be of one type with its level coincident with the shallowest donor level, and its concentration D equal to the sum of the separate donor concentrations. As temperature is increased all these donors empty their charge into the conduction band in a similar way provided their energy spread is not great. Calculations indicate this procedure gives the donor and acceptor concentrations within accuracies of 5% and 30% respectively.

Case II:

The low temperature Fermi level is not coincident with the shallowest donor level. It is presumed that it lies at donor D_2 which is deeper than donor D_1.

In this case the value of the donor concentration obtained by fitting to a two impurity model does not include any of the donors lying above the low temperature Fermi level. Donors located above this level are empty at all temperatures and cannot contribute to the carrier concentration as the temperature is increased. Therefore they do not contribute to the temperature dependence of the measured quantity. In addition their overall presence is not observed because the occupation of the acceptors is also independent of temperature. The neutrality condition

$$\eta(T) + A^- = D_1^+ + D_2^+(T)$$

can be rewritten by grouping the temperature independent terms.

$$\eta(T) = D_2^+(T) - (A^- - D_1^+)$$

Fitting the two impurity model to such a material will give apparent donor and acceptor concentration, D_2 and $A-D_1$ respectively. However, the true donor and acceptor concentrations are $D_1 + D_2$ and A respectively.

2.1.3. Data Analysis. Data was analyzed using one of two techniques.

Approximate graphical fits to equations (A9) through (A12) were made when the quantity or quality of the data was low.

Least squares best fits were obtained using the exact equation (A8). This was done using the main program GLSWS[8] and appropriate subroutines written for fitting to equation (A8).

2.1.4. Experimental. Starting material for all of these experiments was 100 ohm-cm, n-type float-zone silicon grown by Dow Corning. Wafers 0.020 in. thick were alloyed with lithium at 350°C for ten minutes using the paint-on technique. About 0.001 in. was lapped from the alloyed surface prior to a one hour diffusion at 425°C. Lapping reduced the surface concentration of lithium and allowed the final dopant concentration to be varied between 10^{16} and about 10^{13} lithium/cm^3. The homogeneity of the doping introduced in this way has been measured by the four point probe technique.[9] Homogeneity is presently being studied using samples in the Hall configuration, with consecutive lapping and measurement.

Wafers were then masked and six arm Hall samples were cut by sandblasting. After etching in "white etch" (3 HNO_3:1HF), the contact areas were sandblasted and nickel plated by electroless deposition. Leads were soldered using indium metal. Measurements of current-voltage characteristics as a function of temperature in the two contact configuration showed the current contacts were ohmic at all temperatures other than those near 80°K. Four contact measurements showed that the electrical properties of the silicon outside of the contact region were unaffected by the properties of the contacts. This was not true when PbSnSb solder was used instead of indium.

The influence of surface preparation on Hall measurements was checked. A sample was measured with first etched, and then sandblasted surfaces. No surface effects were found even at low temperature.

Low temperature measurements were made with the sample mounted in vacuum on the conduction cooling tail of a helium dewar. In order to allow the temperature to be varied, the sample was not mounted directly on the tail. Instead it was mounted to a sapphire substrate which was soldered to a copper sample holder. This was suspended from the tail by a small diameter brass rod. An electric heater

fastened to the sample mount controlled the sample temperature which was above the helium boiling point due to a thermal gradient in the brass rod. A Princeton Applied Research TC 100.2AR current source was used to power the heater. Temperatures were stable to within 0.1%.

Hall voltages were measured in all four possible permutations of field and current directions in order to average out effects due to contact potentials and constant thermal gradients in the sample. The magnetic field dependence of the Hall constant was determined at several temperatures in order to be sure that all measurements were indeed made in the low field regime. Voltages were measured with a Leeds & Northrup K3 potentiometer in combination with a Keithley 610B electrometer. With this system measurements were limited to sample impedances of 10^{10} ohms because of cable capacitance and electrical isolation problems. At the time of this work only one sample could be accommodated. Since then, modification has been made to accomodate up to three samples, thereby allowing control samples to be included.

Two thermometers were mounted on the sample holder for the measurement of temperature. A platinum resistance thermometer made by Microdot, Inc. was used for temperatures above 80°K. It was calibrated using the boiling point of nitrogen and room temperature as fixed points. The second thermometer was a 100 ohm, 1/10 watt Allen Bradley carbon resistor. This was calibrated using the boiling points of helium and nitrogen, and the vapor pressure of hydrogen and neon. It was also checked against a calibrated germanium resistance thermometer and found to agree within 1% over the range 4°K to 80°K. Thermometer resistances were measured using an A. C. bridge dissipating less than one microwatt in the thermometer.

2.1.5. Results. The results of three experiments are reported here. Each experiment contributed to the formulation of the succeeding experiment. As a result of equipment improvements the data of the last experiment is of greater precision than that of the first two experiments. The experiments were performed under the following conditions:

(1) 300°K irradiation and annealing of heavily doped Si(Li).

(2) 80°K irradiation and 300°K annealing of moderately doped Si(Li)

(3) 80°K irradiation and primarily 300°K annealing of lightly doped Si(Li).

These three experiments will be discussed separately under the headings below.

I. 300°K Irradiation - Heavy Doping

A sample of silicon doped with 3.7×10^{16} lithium/cm^3 was measured before and 30 minutes after a 300°K irradiation of 10^{16} 1 MeV electrons/cm^2. After 140 hours at 300°K it was measured again.

Since the quality of this data was marginal, no correction for Hall factor was made. At this dopant concentration the Hall factor should have a value of 1 above 100°K and increase to about 1.4 at lower temperatures.[6] The data was reduced using the approximate expressions (A9), (A11), and (A12) of Appendix A instead of the exact formula, (A8). Carrier concentration and Hall mobility are shown in Figs. 2 and 3 respectively before and after irradiation. Results after 140 hours were unchanged from the post-irradiation values and are not plotted. The parameters obtained from this data are shown in Table 1.

Both before and after irradiation, the slopes of the linear portions of Fig. 2 equal one half the activation energy of lithium. The measured value of the activation energy (d-c) (Table 1) agrees well with the accepted value, 0.033 ev. Since the observed slope is one half the activation energy, from (A11) (Appendix A) it can be concluded that the acceptor concentration is very small before and after irradiation. The knee in the pre-irradiation data of Fig. 2 indicates a transition to the condition of equation (A12) thereby confirming this interpretation. The small acceptor concentration observed before irradiation is not surprising since lithium is known to complex with and remove acceptors during diffusion.[10,11] However, experience with phosphorous doped float-zone material indicates on the order of 10^{16} acceptors should have been created by this irradiation.[12] This would have changed the slope in Fig. 2 by a factor two. Indeed a carrier removal rate comparable to that of Si(P)[12], namely, about 1.2 cm^{-1}, can be seen in Table I, but acceptor generation is absent. In this case carrier removal, that is the change in the quantity D-A, arises entirely from a decrease in donor concentration.

Furthermore the radiation-induced increase in Hall mobility of Fig. 3 indicates that the donors were removed to less efficient scattering centers than isolated single donors.[13] These centers may be neutrally charged. It should be noted that radiation-produced acceptors would have tended to reduce carrier mobility. We were unsuccessful in our attempt to analyze the scattering centers by fitting

TABLE I SILICON PARAMETERS WITH 3.6×10^{16} Li/cm^3 DOPING

	D	A	d − c	g
PRE − IRRAD.	3.6×10^{16}	$\sim 8 \times 10^{13}$	.0328 eV	5
POST− IRRAD.	2.4×10^{16}	$\lesssim 10^{14}$	.0309 eV	8
140 h	$\sim 2.4 \times 10^{16}$	$\lesssim 10^{14}$	.0323 eV	3

Parameters obtained from fitting the data of Fig. 2 to equations A9, A11, and A12. D and A are donor and acceptor concentrations respectively. Low temperature Fermi energy is d-c and g is the donor ground state degeneracy factor.

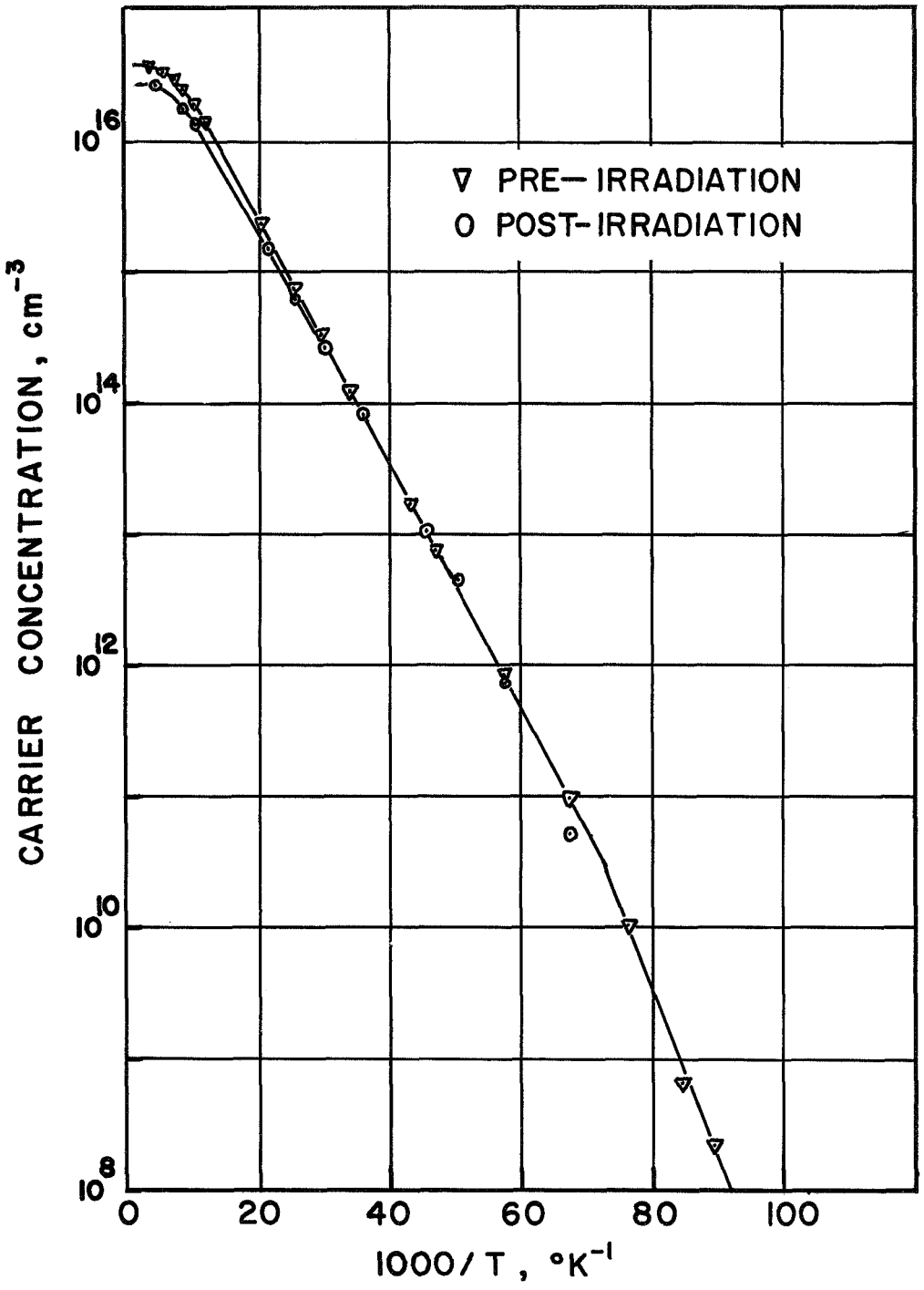

Figure 2 Carrier concentration as a function of inverse temperature for a sample of silicon doped with 3.6×10^{16} Li cm^3 and after irradiation at 300°K by 10^{16} 1 MeV e/cm^2. Data obtained after 140 h at 300°K is unchanged from the post-irradiation result and is not shown.

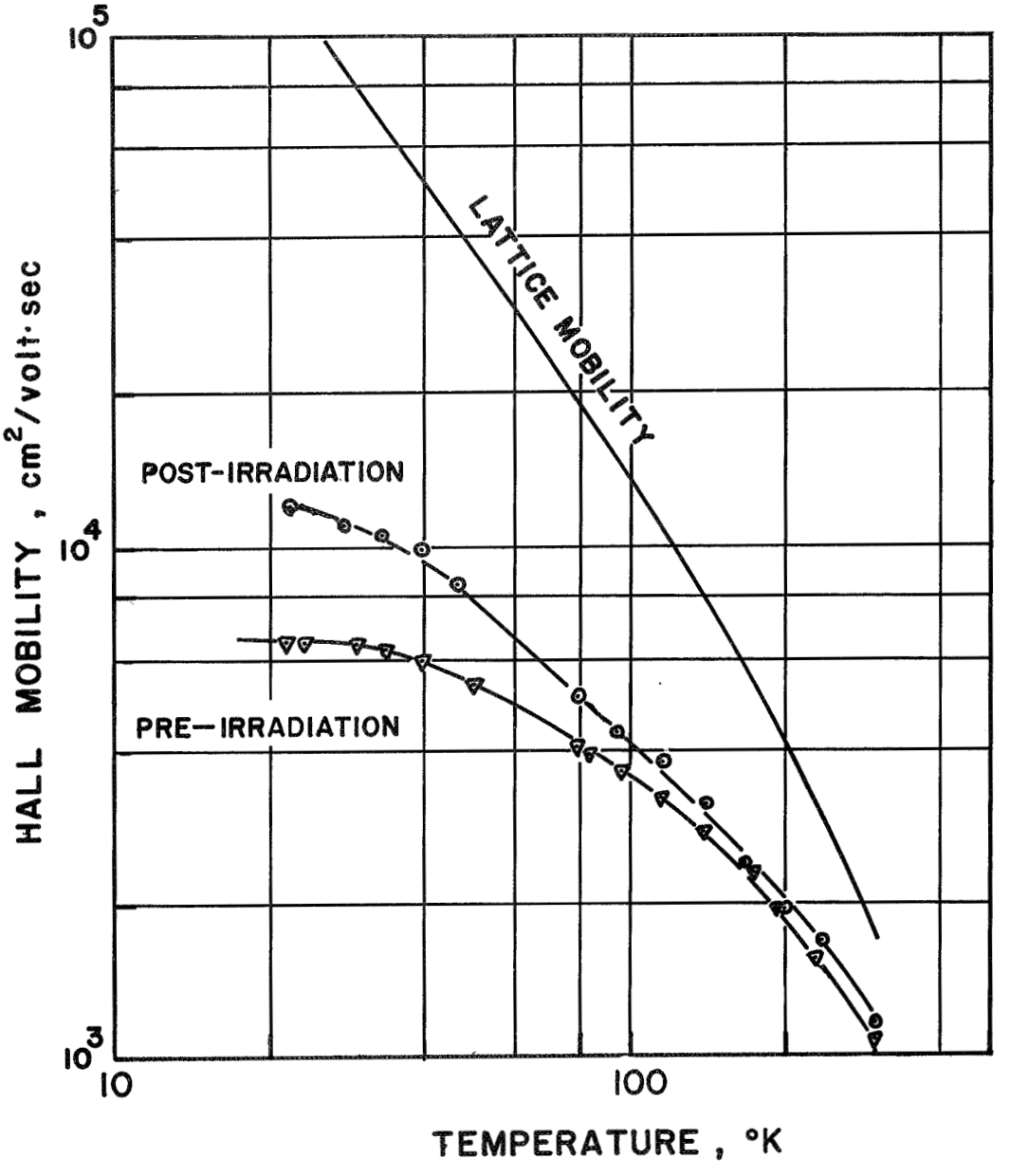

Figure 3 Hall mobility as a function of temperature for the sample of Figure 2. Lattice mobility is the mobility expected for pure silicon.

mobility data to each of several theories. This failure may have been due to inappropriate physical models or the lack of a correction for the Hall factor. Experience indicates however, that even the simplest theories of Hall mobility can be applied to real materials with limited success.

This experiment revealed that annealing of damage in heavily doped float zone material must occur during 300°K irradiation itself. In order to observe the damage produced, irradiation must be done at low temperature where lithium is immobile.

II. 80°K Irradiation - Moderate Doping

This sample, containing 4×10^{15} lithium/cm^3, was measured before and after irradiation at 80°K with 10^{15} 1 MeV e/cm^2. After 130 hours at 300°K it was remeasured.

The data, which was of better quality for this sample, was reduced using the fitting program. The pre-irradiation data did not give as good a fit as did the two subsequent measurements. This affected primarily the pre-irradiation values of D and A. Again no correction for Hall factor was made. The carrier concentration and parameters obtained from curve fitting are shown in Fig. 4 and Table II respectively. Hall mobility was essentially unchanged throughout the set of measurements because the low degree of damage did not greatly change the number of charged scattering centers.

The knee shown in Fig. 4 again indicates that acceptor concentrations were much less than donor concentrations (cf. Table II). In this case however, the indicated activation energy is approximately 0.028 ev instead of 0.033 ev. Such behavior was found in a number of samples prepared in the same way as those giving the proper activation energy. (Similar results are reported in the literature.)[11] Further work is being done to discover the reason for this low value. This anomalous behavior weakens the conclusions concerning basic mechanisms one can make from this sample. However, the primary point of interest is not affected. This is that acceptors are generated by irradiation at 80°K and the knee moves to higher temperatures. If a larger dose had been used the knee would have moved to sufficiently high temperatures that it would not be evident at all and the apparent slope would have increased by a factor of two. On annealing, the acceptor concentration was returned to nearly its original value. Due to reduced damage rates at 80°K the number of damage centers was very small compared to the lithium concentration. As a result, no change in the lithium concentration was observed from the damage and annealing processes.

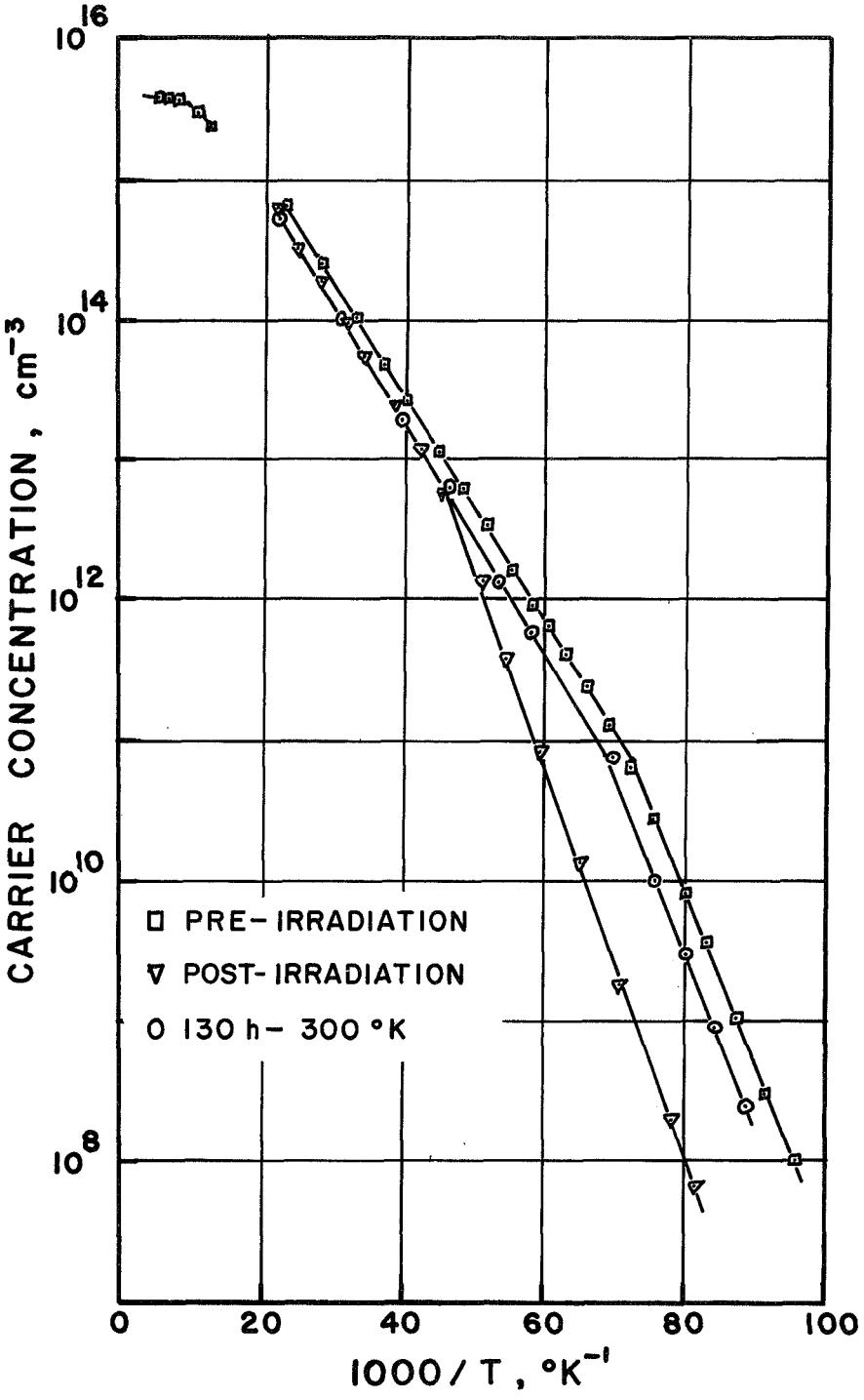

Figure 4 Carrier concentration as a function of inverse temperature for a sample of silicon doped with 4×10^{15} Li cm^3, after irradiation by 10^{15} 1 MeV e/cm^2 and after 130 h at 300°K.

TABLE II SILICON PARAMETERS WITH 4×10^{15} Li/cm^3 DOPING

	D	A	d – c	g
PRE – IRRAD.	$\sim 4 \times 10^{15}$	$\sim 3 \times 10^{10}$	·0284 eV	3
POST– IRRAD.	$4{\cdot}0 \times 10^{15}$	$9{\cdot}8 \times 10^{12}$	·0265 eV	9
130 h	$4{\cdot}0 \times 10^{15}$	$5{\cdot}4 \times 10^{10}$	·0284 eV	7

Parameters obtained from fitting the data of Fig. 4 to equation A8. The pre-irradiation parameters were obtained by graphical methods. The remaining parameters were obtained by machine.

This experiment confirms that separation of the damage and annealing processes in float-zone silicon requires that irradiation be performed at low temperature.

III. $80^{\circ}K$ Irradiation - Light Doping

A sample of 100 ohm-cm float-zone silicon was doped with lithium by diffusion to a total donor concentration of 10^{14} n/cm^3. The ratio of the concentration of lithium to that of phosphorus was about one to one. Following an initial measurement the sample was irradiated at $80^{\circ}K$ with 4×10^{14} 1 MeV e/cm^2 and remeasured. Subsequently it was remeasured after annealing at $200^{\circ}K$ to remove intrinsic defects,[13] and after five periods of increasing duration at $300^{\circ}K$. The resultant data were fit to a two impurity model with four adjustable parameters using the method of least squares.[8]

(a) Measurements Below $100^{\circ}K$

The results obtained from measurements made below $100^{\circ}K$ are discussed first. Experimentally determined electron concentration as a function of inverse temperature is shown in Fig. 5. Electron concentration changed over eight orders of magnitude as the temperature changed from $100^{\circ}K$ to $14^{\circ}K$. The low temperature limit was set by the inability of the apparatus to measure potentials from a source whose impedance was greater than 10^{10} ohms. The slope of the curves in the linear portion represents the Fermi level at low temperature. Comparison of these curves shows the Fermi energy moved deeper into the gap as the experiment proceeded. The value of the electron concentration at high temperature equals D-A and decreased on annealing at $300^{\circ}K$. The form of this decrease was in agreement with the carrier removal studies by Carter.

Fits of the two impurity model to this data gave the parameters in Table III. From left to right the columns indicate apparent donor and acceptor concentrations, low temperature Fermi level and donor degeneracy factor.

Table III shows degeneracy factors (g) as high as 34 where normally 1 would be expected for a single donor measured under the best conditions. Clearly the parameter g lacks physical significance. To check this point two things were done. First, a sample of 30 ohm-cm Si(P) was measured and a two impurity fit was applied. A value of $g = 1.3$ was obtained using the least squares program. Secondly, carrier concentration

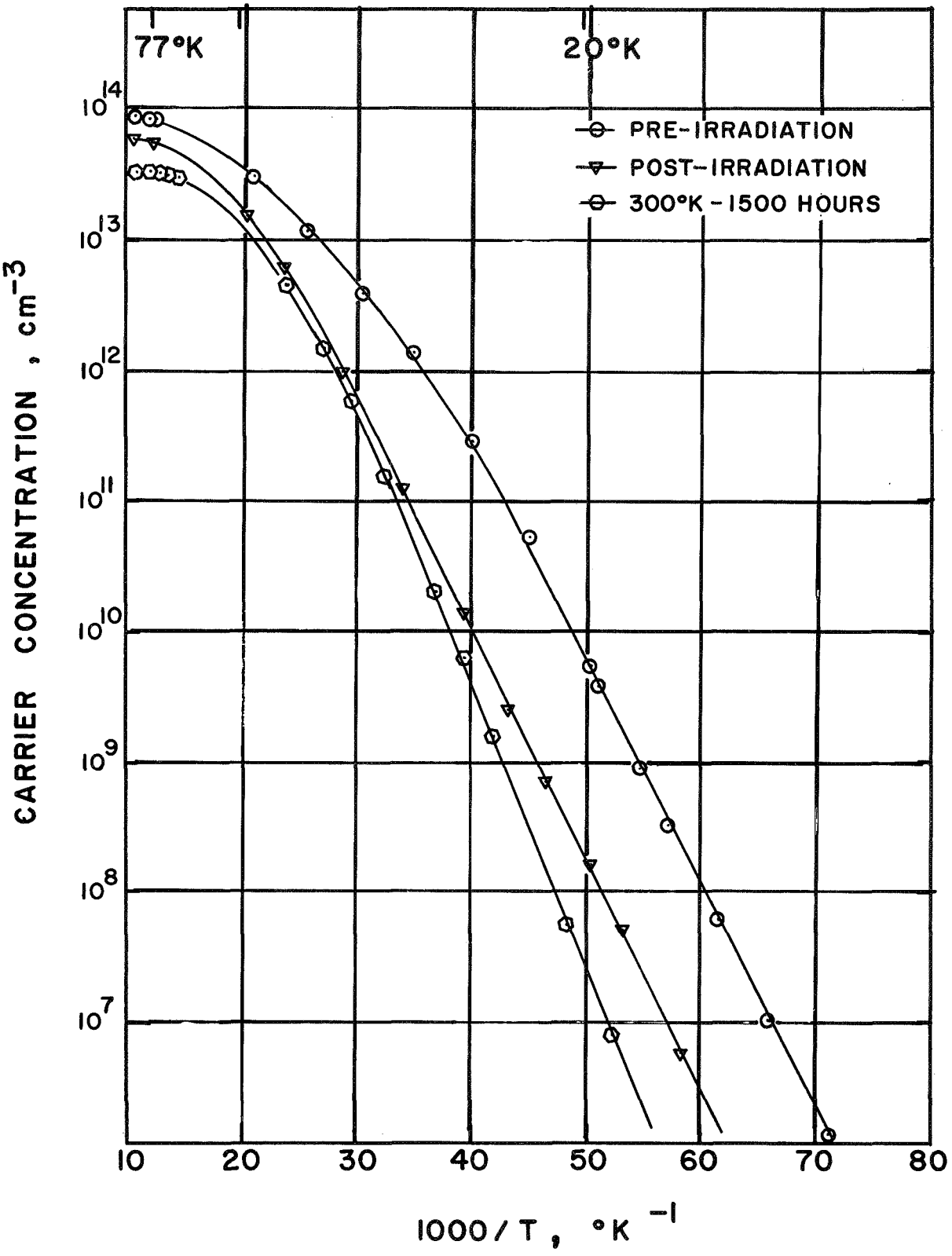

Figure 5 Carrier concentration as a function of inverse temperature for a sample of silicon lightly doped with lithium. Only three curves are shown out of a set of eight actually measured. Irradiation was performed at 80°K.

TABLE III SILICON PARAMETERS WITH $<1 \times 10^{14}$ Li/cm^3 DOPING

	D	A	d − c	g
PRE-IRRAD.	9.3×10^{13}	1.4×10^{12}	.0319	22
POST-IRRAD.	8.0×10^{13}	1.8×10^{13}	.0322	34
1.5h at 200°K	7.4×10^{13}	2.2×10^{13}	.0323	18
4h at 300°K	6.5×10^{13}	1.5×10^{13}	.0337	21
61h at 300°K	6.1×10^{13}	1.7×10^{13}	.0346	16
114h at 300°K	4.7×10^{13}	5.1×10^{12}	.0375	17
272h at 300°K	4.3×10^{13}	5.6×10^{12}	.0375	16
1460h at 300°K	3.7×10^{13}	1.8×10^{12}	.0406	10

Parameters obtained from fitting the data obtained from the lightly doped sample of Si(Li). These values were obtained by machine fits to equation A8.

as a function of temperature was calculated for several imaginary samples doped with three impurities. When the two impurity model was fitted to these, degeneracy factors ranging from 1 to 6 were obtained. Evidently the behavior of the parameter g is related to the approximate nature of the two impurity model. These same imaginary samples indicated that the two impurity parameters D and A were reliable to within 5% and 30% respectively.

Figure 6 is a plot of the low temperature Fermi energy (d-c) as a function of apparent donor concentration (D). The points shown were obtained in sequence starting at the upper right. Figure 6 shows pinning of the Fermi level at 1.0 and 2.0 meV above the optical excitation energies of the Li^+ and LiO^+ donors respectively.[15] The difference between the optical and thermal values of the excitation energy for phosphorus is about 1.0 meV[16,17]. This is comparable to the differences seen here for Li and LiO, thereby identifying the active donors in this sample. This data indicates the thermal activation energy for LiO^+, which has not been measured previously, as approximately 0.0375 eV.

Figure 7 shows the dependence of apparent donor and acceptor concentrations as obtained from fits to the two impurity model. Figure 6 however showed that the low temperature Fermi level had passed through both the Li and LiO donor levels. As a result of this the two impurity parameters D and A will be decreased from their true value by an amount equal to the concentration of the donor level(s) passed through. Thus the overall decreases in D and A of Fig. 7 may be only apparent and caused by an acceptor concentration that is increasing with time. No mechanism is known that could cause such an increase.

A more reasonable explanation presumes that indeed the acceptor concentration was decreasing as was the donor concentration. If the acceptor concentration was decreasing, the Li^+ concentration must have become very small as the Fermi energy passed through it. If such were the case there would be no defect counting error. A similar argument would obtain for the passage of the Fermi level through the LiO^+ level. This argument agrees in all details with the accepted concepts regarding lithium complexing and neutralization of defects. The evidence given here is not sufficient to prove these concepts however.

(b) Measurements Above 100°K

As the temperature is increased above 40°K the Fermi energy tends to move downward toward the center of the gap. At 300°K it can be as low as 0.3 eV below the bottom of the conduction

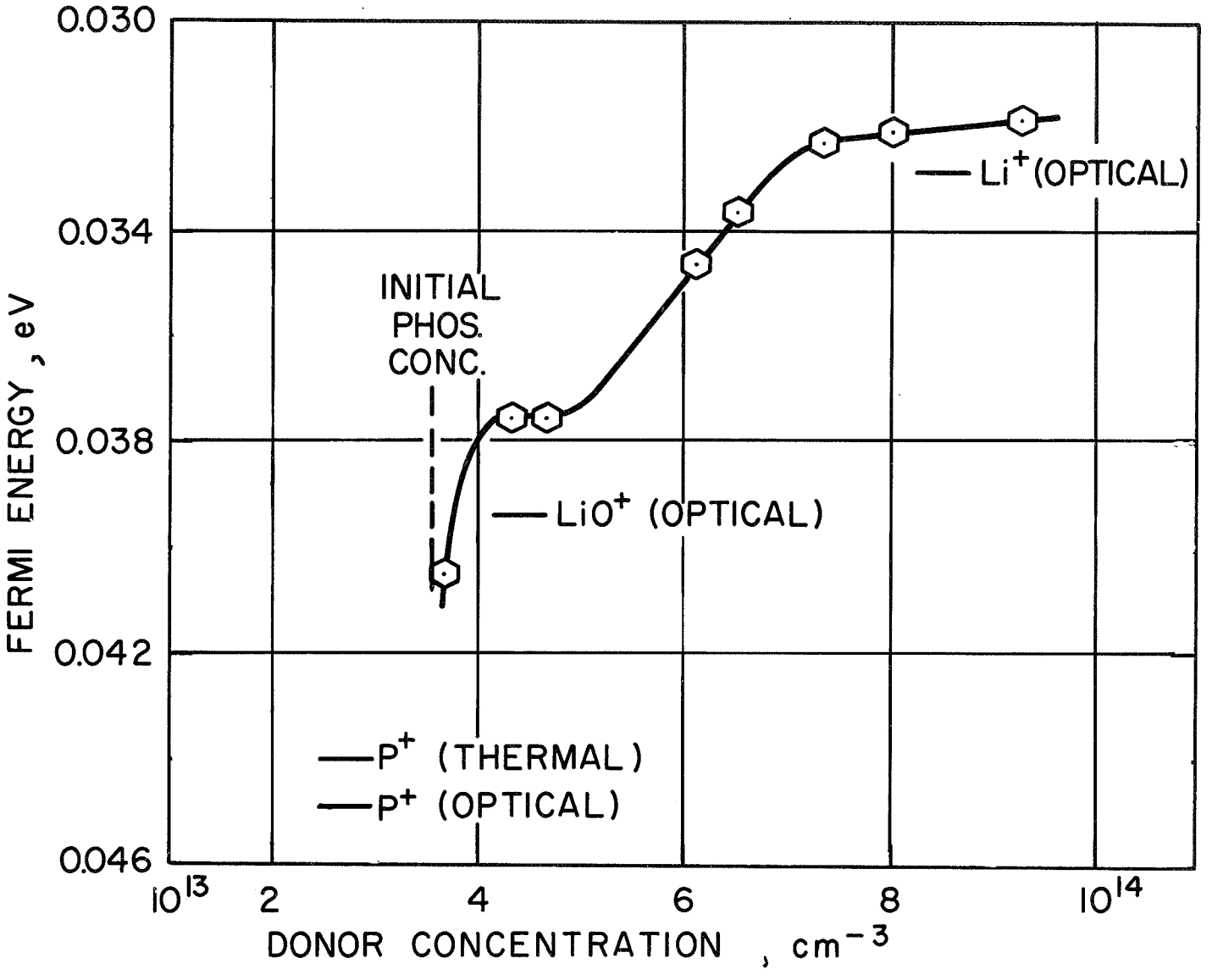

Figure 6 Low temperature Fermi level moved lower into the forbidden gap as the apparent donor concentration in Table III decreased. The points were obtained in a sequence starting at the upper right.

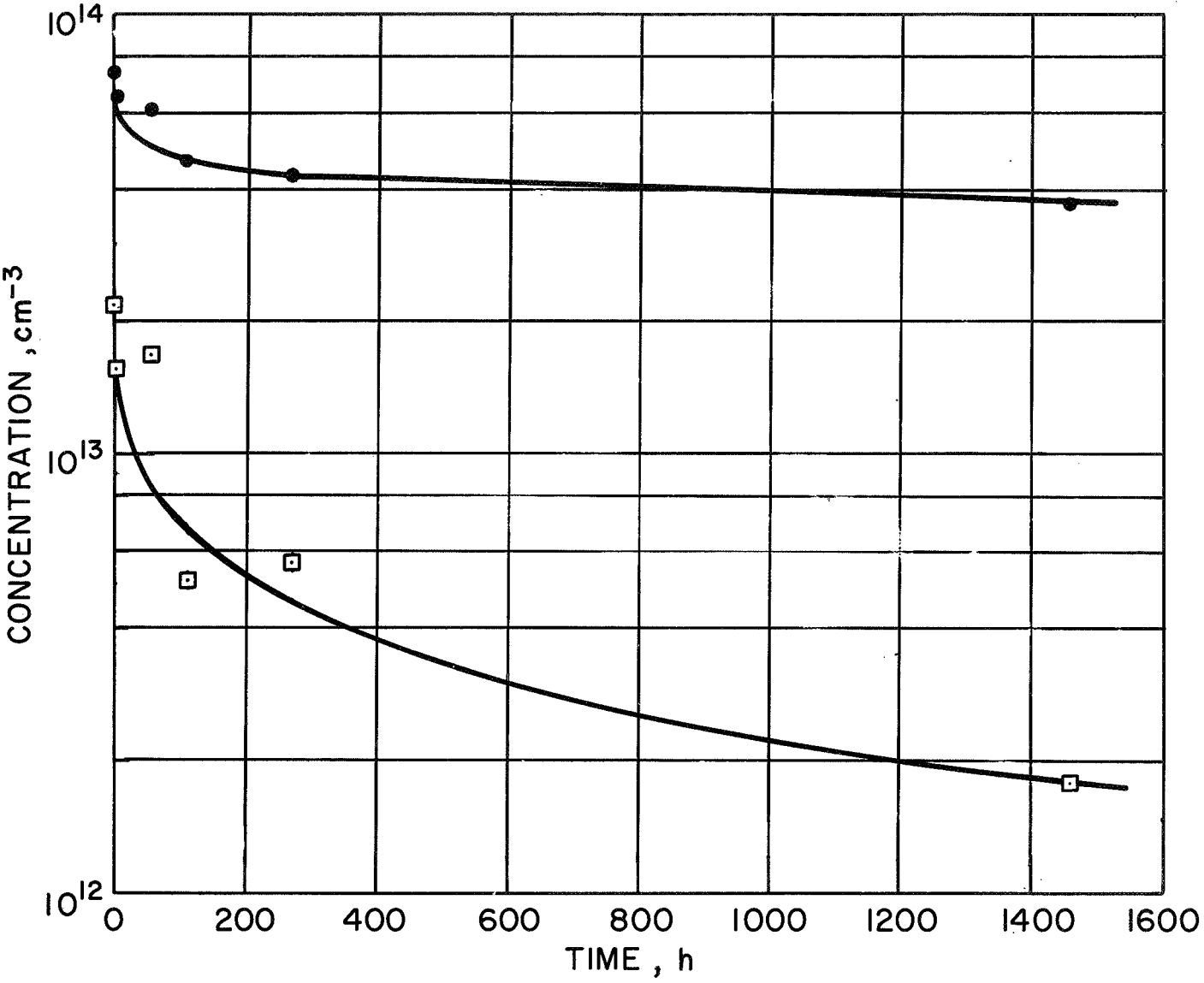

Figure 7 Values of apparent donor and acceptor concentration obtained from the two impurity model decreased with time of annealing at 300°K. The upper and lower curves represent the donor and acceptor concentrations respectively.

band. At such high temperatures the concept of filled versus unfilled loses meaning. Suffice it to say that if the Fermi level passes through a level as it moves downward the population of that level will change and will thus produce a structure in the Hall data. Corrections for the Hall factor were necessary and were made using the Hall factor determined from the data taken before irradiation.

Structure due to A centers at 0.185 eV below the conduction band was not observed in measurements made after 61 hours at 300°K. Structure due to a deep level was observed however and its effect on the Hall data is shown in Figure 8. This structure was not seen prior to irradiation. The various curves were taken at the indicated annealing times. Analysis indicates a concentration of about $1.5 \times 10^{13}/cm^3$ and is apparently independent of annealing time. This level may well have been present immediately after irradiation. The depth of this level can be seen from Fig. 9. The dotted lines are carrier concentrations calculated for several values of deep level ionization energy. Apparently the shape of the data agrees well with theory and the level is approximately 0.15 eV below the conduction band. Since there was no control sample the importance of Li to this level is an open question. The fact that it was not seen in the pre-irradiation Hall measurement indicates however that it was introduced during or subsequent to the irradiation. Structure due to the A center would be near the 0.19 eV curve and is clearly not observed for annealing times greater than 61 hours.

2.1.6. Conclusions

The purpose of this work has been to find the conditions under which the damage and annealing processes can be separated. The first two experiments served this purpose.

The third experiment was intended to show the changes in lithium and damage center concentrations upon annealing at 300° K. Due to the motion of the Fermi level a unique interpretation of the observed donor and acceptor concentration behavior was not possible. The motion of the low temperature Fermi level did demonstrate the presence of the LiO donor and indicate its thermal activation energy. This experiment also indicated the value of Hall measurements made above 100°K for monitoring deep defect concentrations. Exploitation of these measurements for lightly irradiated samples with only a few kinds of deep centers may help identify the centers reacting with lithium and perhaps the final products.

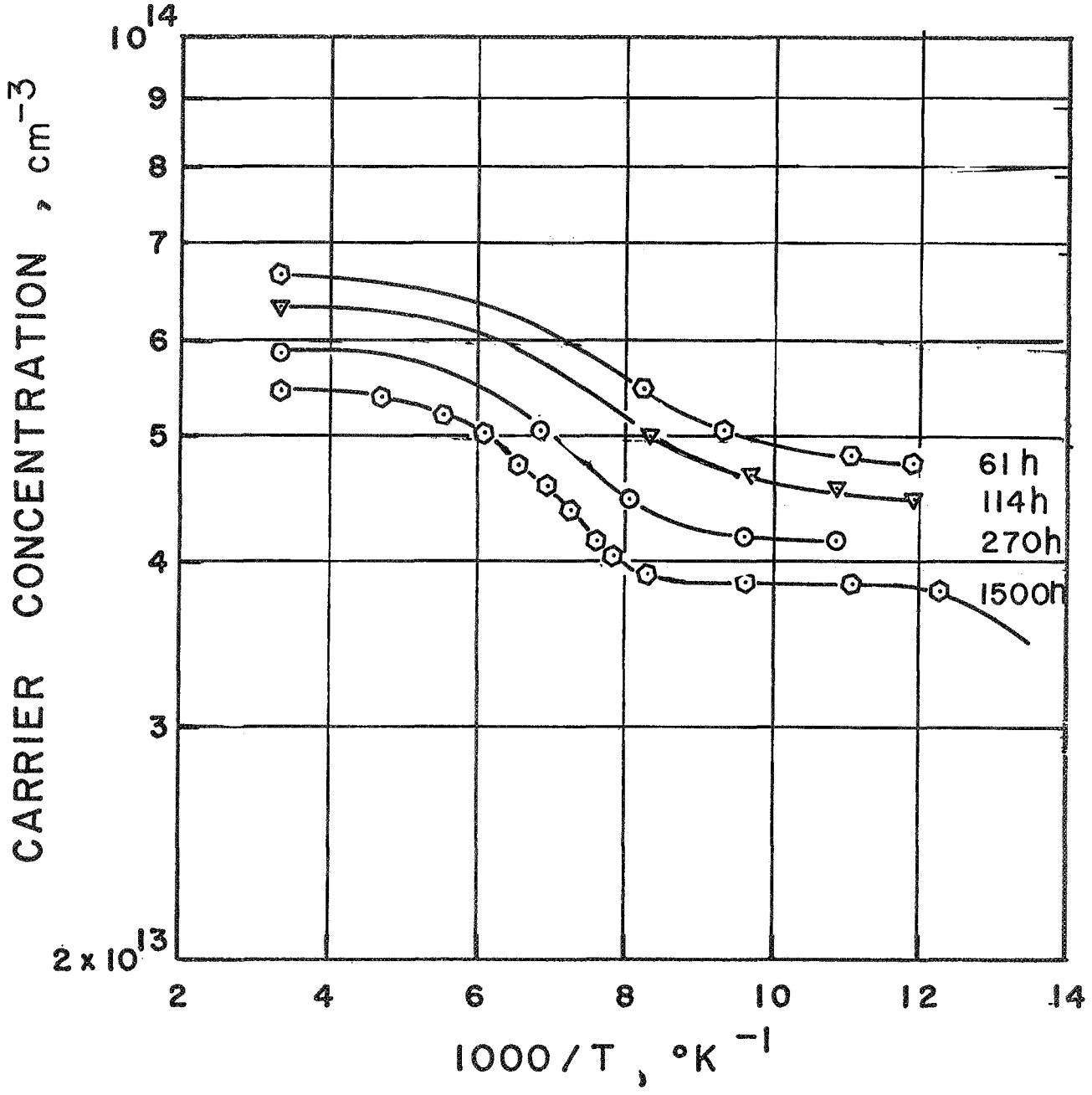

Figure 8 The family of curves shows the dependence of the deep level structure upon time of annealing. The difference in carrier concentrations between the plateaus of each curve is the deep level concentration. No change in this concentration with annealing is observed.

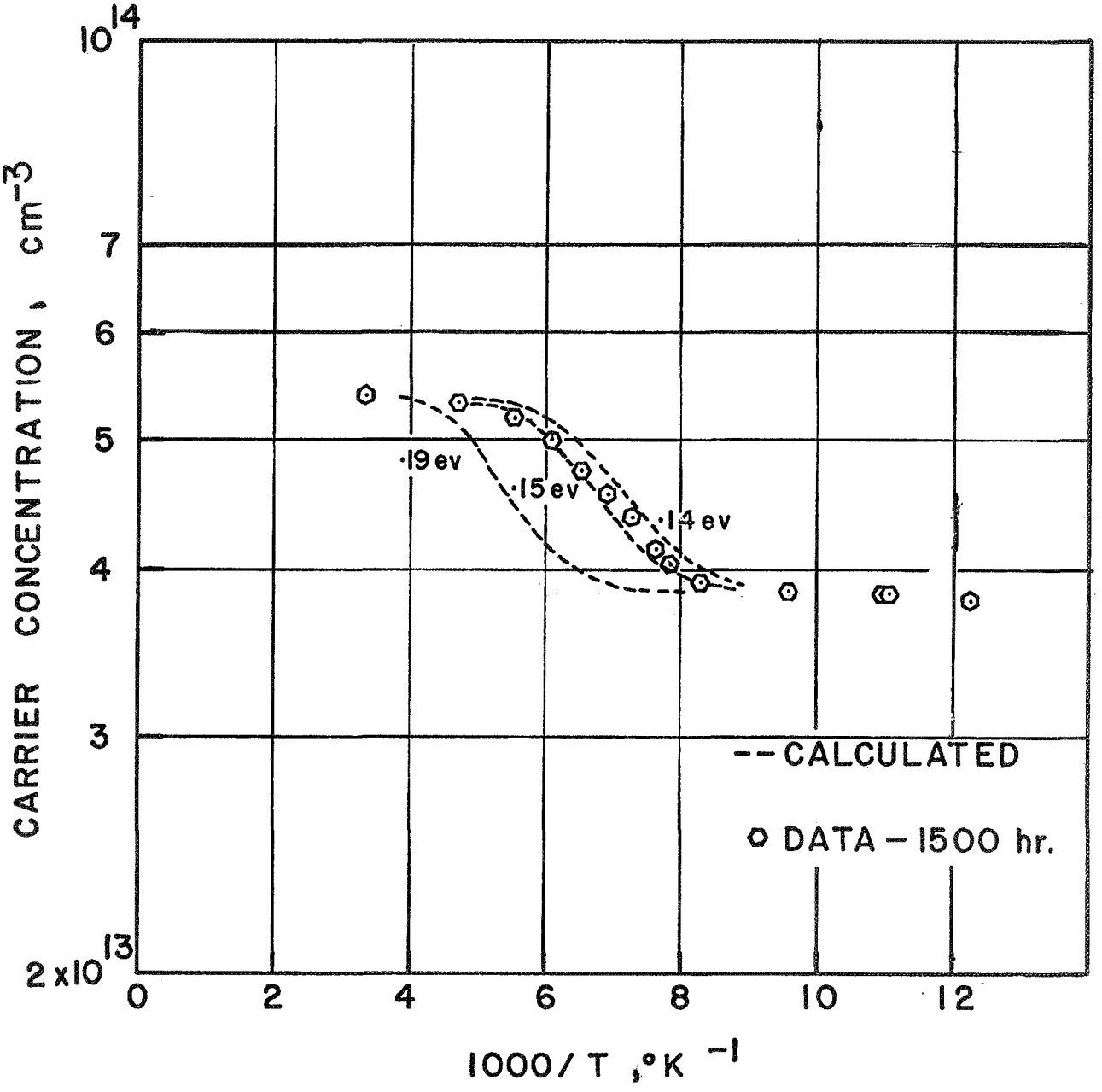

Figure 9 Comparison of the observed deep level structure to three impurity theory for three values of deep level activation energy.

2.2 Low Flux Gamma Radiation of Lithium-Diffused Solar Cells

2.2.1. Introduction

Lithium introduced as an added impurity in p/n solar cells gives to the cell the property of self-annealing of radiation damage. The exact degree of such recovery depends on the initial physical properties of the cell, and on environmental conditions external to the cell. The predominant internal factors are the concentration of lithium, oxygen, and primary dopant. The important external factors are ambient temperature and radiation dose. Another factor which has not been resolved is whether there is a dose rate dependency of annealing. Most experiments have been performed with high flux rate accelerators which generate radiation at a rate several orders higher than found in space radiation. Thus it is quite important to study lithium-diffused solar cells for a flux rate dependence, to ensure the validity of data from high flux studies.

2.2.2. Phase I - Continuation of Goddard Space Flight Center Experiment

This experiment was begun in June 1967 under the direction of P. Fang, then at Goddard Space Flight Center, NASA. The contractual work was performed by Electro-Mechanical Research, Inc. under NASA-GSFC Task 713-2220. The EMR work was completed in August 1968 and the cells were transferred to NRL for continuation of the experiment for as long as the study was useful.

The final report [20] of the EMR work was followed by a paper by Fang. [21]

The experiment consisted of gamma irradiation of a number of lithium and conventional solar cells in two evacuated chambers in a Co^{60} swimming pool source. At the time of transference to NRL the various cells had received a total dose up to a maximum of 3.74×10^{15} 1 MeV e/cm^2 equivalent in fourteen months.

About half the cells were illuminated by tungsten light during irradiation while the rest were dark. No temperature control was attempted. Because of the water temperature variation at the gamma source, the cells also varied over a temperature range in one chamber from 30 to 40°C and in the other chamber from 55 to 75°C. Daily readings were made of the temperature, vacuum, and illumination voltage.

The experiment was continued for five months at NRL, during which time the cells received an added 5.5×10^{14} 1 MeV e/cm^2 equivalent dose. Measurements of the I-V curves were made monthly on every cell under a tungsten light source of 100 mW/cm^2 solar equivalent with a 3 cm water filter. For the measurement the cells were removed from the gamma source and held in dry ice except for a 15 minute period at the time of measurement.

Our tungsten light gave I_{sc} values about 12% less than the EMR measurement. Thus the lack of initial experimental data, uncontrolled variation in cell temperature, and insufficient samples of each type prompted the termination of this phase of the work.

It is not possible to establish specific values of significant differences between cell types from the data of this experiment. A few general conclusions can be made with respect to the NRL portion of the work.

(1) The float-zone lithium diffused cells were almost stabilized with respect to further radiation damage after a dose of 4×10^{15} e/cm^2, whereas the Lopex and crucible grown lithium cells were still degrading slightly.

(2) The n/p commercial cells continued to degrade at a rate equal to the worst of the lithium cells.

(3) Tungsten efficiencies for lithium cells at the dose of 4×10^{15} e/cm^2 ranged from 4.6 to 7.7%.

(4) The most important fact is that there was a continuing damage rate in the lithium cells which extended throughout the entire twenty months of the investigation.

2.2.3. Phase II - New Experiment at NRL Co^{60} Gamma Pool

The low flux Co^{60} gamma irradiation experiment was redesigned to improve the sample statistics and thereby yield more quantitative results. One of the criticisms of the first phase study was that there were too few samples of each type, and too many experimental variables. For the new phase, the number of samples was increased to five of each type to irradiated under each set of conditions, and three samples of each type to be used as controls. The need for temperature control had been made evident from the first phase study, where cell temperatures had varied over a range of 15 or 20°C. A decision was made to irradiate all solar cells while illuminated with as intense a light as could be used in the confined space of the irradiation cans. This turned out to be less than 0.5 equivalent solar constant.

The experiment sample matrix is shown in Table IV. The lithium diffused cells were made by Heliotek and obtained through the Jet Propulsion Laboratory. The n/p commercial cells were obtained directly from Centralab. The measured efficiencies of these cells are listed in Table V. Three stainless steel chambers are used for the Co^{60} gamma irradiation. These are cylindrical cans about 3 in. diameter and 9 1/2 in. long. The solar cells are held against brass plates by spring clips at the main bus bar (Fig. 10). Electrical contact is made to the cell through the plate and the spring clips. Each cell is loaded with a ten ohm resistor.

Illumination is provided by five automobile lamps in each can as shown in Fig. 11. The original plan called for a quartz envelope tungsten wire filament bulb, to be specially constructed at NRL. Several bulbs were made and tested, but proved to be short-lived, probable because of excessive heat build up. The automobile bulbs have performed satisfactorily for almost 3 months of continuous use. During the trial tests it was discovered that when the irradiation cans were evacuated with a fore-pump as the lamps were on, the heat build-up of the lamps was great enough to melt the solder connections. Therefore the decision was made to fill the cans with argon during the experiment to provide for heat conduction while maintaining an inert atmosphere. Presently the cans are vacuum pumped each month after loading the cells, and then filled with argon to one psi pressure.

The cell temperatures are maintained by controlling the temperature of the brass plate through a combination of electric strip heaters and water-carrying tubing soldered to the back of the plate. One can is held at 30°C, and two cans are held at 60°C with a variation of ±1°C. Temperatures of the plates are measured by iron-constantan thermocouples and continuously recorded on a chart-recorder. The strip heater thermostats are a meter-relay type made by Assembly Products, Inc.

The cells are removed from the gamma source at approximate monthly intervals for measurement of the I-V curve under one sun illumination from a Spectrolab X-25L solar simulator. During this time they are kept at dry-ice temperature except for handling time in and out of the chambers, and about 15 minutes for measurement.

The maximum efficiency measured after the first two months of irradiation are shown in Table VI. The control cells (all non-irradiated cells held at 60°C) show good stability, with the exception of the high lithium concentration float-zone cells. Thus they are useful for indicating the

TABLE IV Co^{60} EXPERIMENT SAMPLE MATRIX

Cell Type	Other Data	Number Irradiated		Controls
		30°C, Illuminated	60°C, Illuminated	60°C, Illuminated
Lithium p/n Float Zone	Low Li Concentration	5	5	3
	High Li Concentration	5	5	3
Lithium p/n Crucible	Low Li Concentration	5	5	3
	High Li Concentration	5	5	3
n/p Commercial	Centralab	5	5	3

All lithium cells were made by Heliotek.

Cells are gamma-irradiated in tungsten, illumination and have 10 ohm load resistors, developing a load voltage of 0.20 to 0.24 volt. The control cells are also resistor loaded.

TABLE V

AMO EFFICIENCY OF SOLAR CELLS*

Lot. No.	No. of Cells	Type of Silicon	Average Efficiency
H 9	15	High Li conc. Float zone	9.0
H 5	15	Low Li conc. Float zone	9.8
H 6	15	High Li conc. Crucible-grown	8.9
H 2	15	Low Li conc. Crucible-grown	9.9
C	20	Boron doped Crucible-grown	10.5

*Measured at 25°C with Spectrosun X-25L solar simulator at 140 mW/cm^2 AMO.

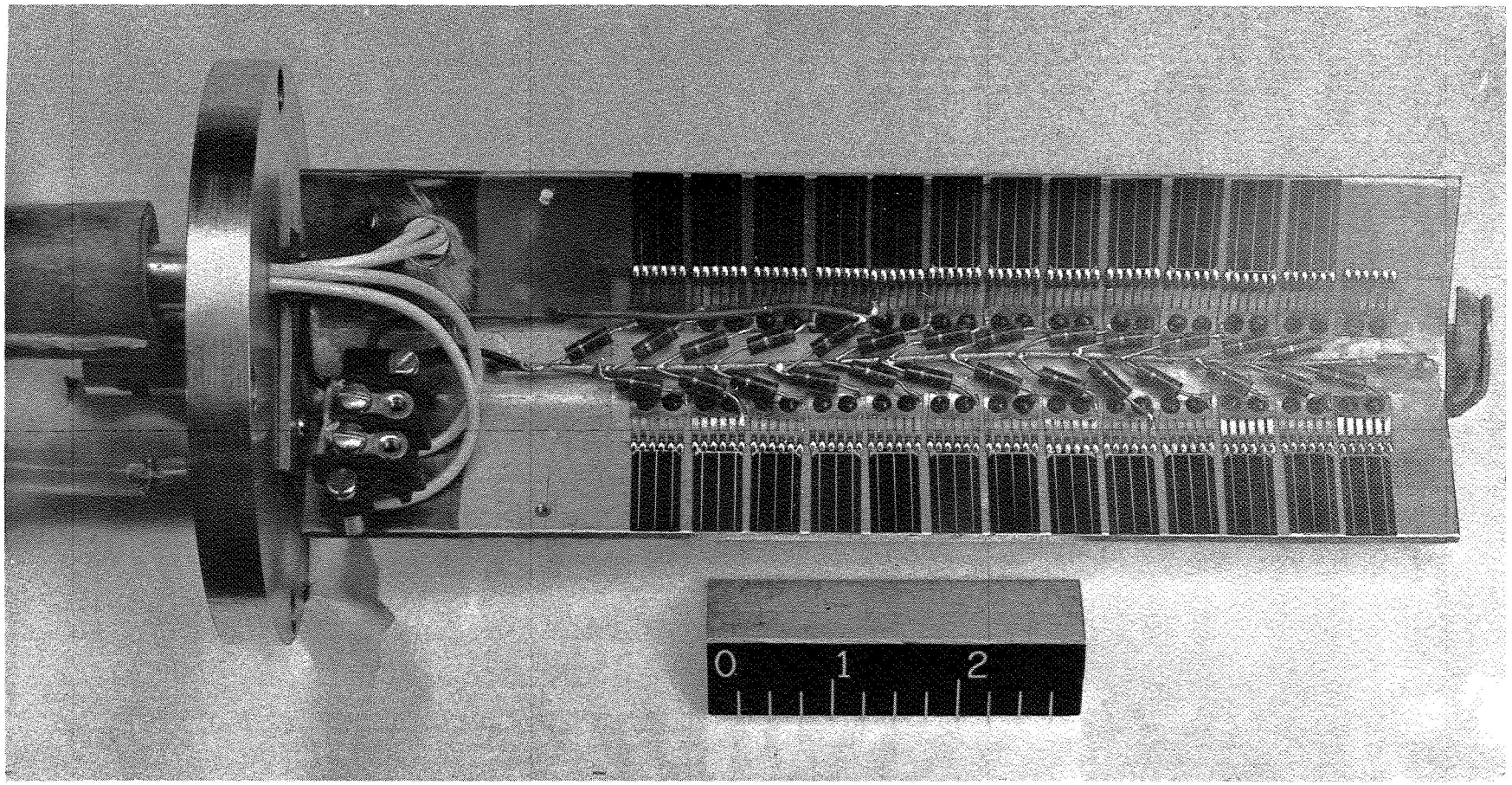

Figure 10 Solar cells are held to brass plate by pressure contacts for Co^{60} gamma irradiation. Each cell is loaded by a ten ohm resistor.

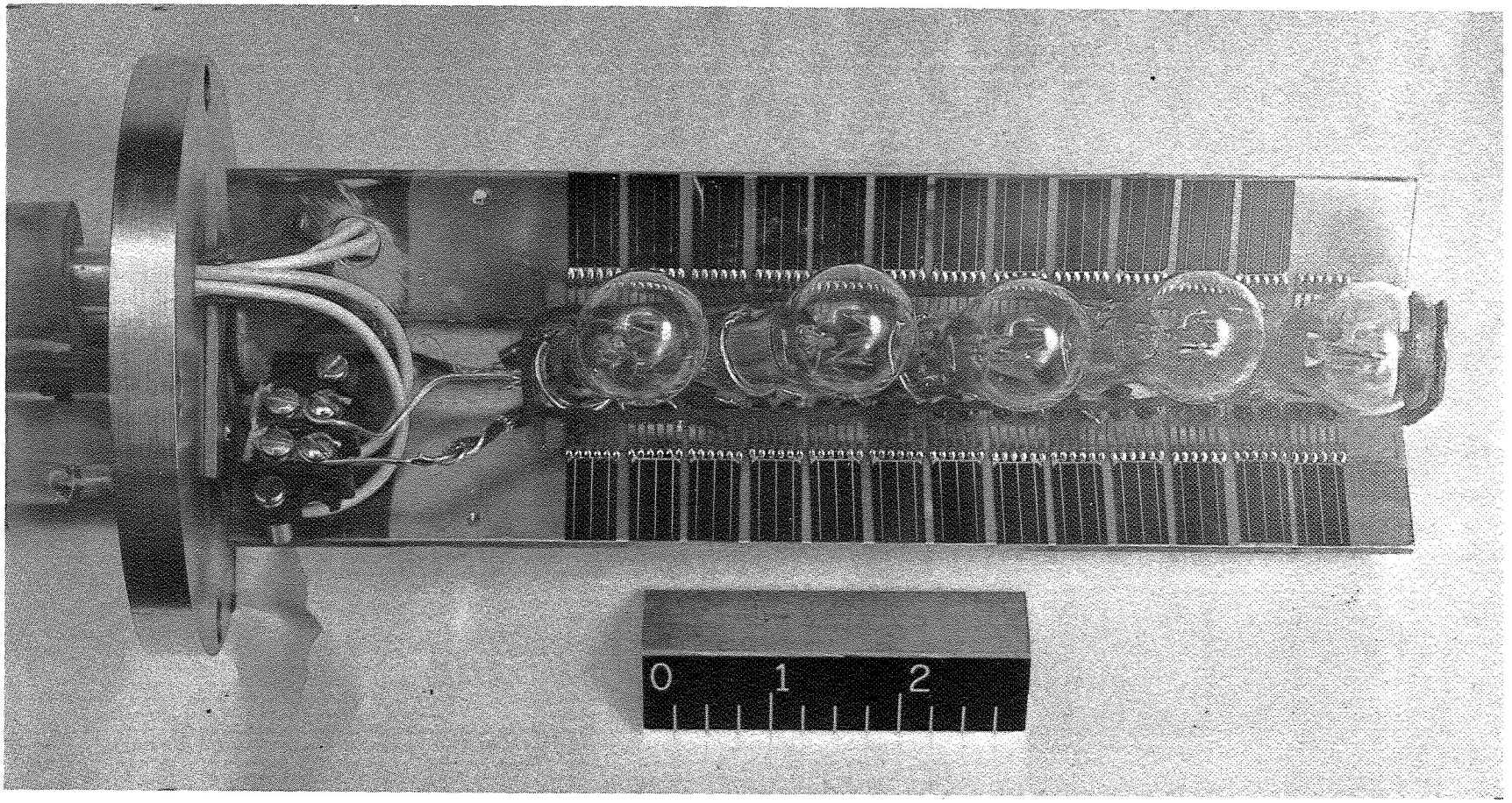

Figure 11 Five 12 volt lamps operating at 1.1 amperes illuminate the solar cells for the Co^{60} gamma experiment.

TABLE VI

AMO EFFICIENCY OF Co^{60} IRRADIATED SOLAR CELLS

Cell Type	AMO MAXIMUM EFFICIENCY AT 25°C AFTER COBALT - 60 DOSE (ROENTGENS)		
	0	3.12×10^6	6.01×10^6
Low Li, CG			
60°C No rad.	9.9	9.8	9.8
60° Co^{60}	9.9	9.6	9.6
30° Co^{60}	10.0	9.6	9.4
High Li, CG			
60° No rad.	9.0	9.0	8.9
60° Co^{60}	8.8	8.6	8.6
30° Co^{60}	8.8	8.6	8.4
Low Li, FZ			
60° No rad.	9.8	9.9	9.8
60° Co^{60}	9.8	8.7	8.3
30° Co^{60}	9.8	8.6	8.3
High Li, FZ			
60° No rad.	9.2	8.8	8.7
60° Co^{60}	9.0	8.5	8.4
30° Co^{60}	8.9	8.6	8.5
B doped, n/p			
60° No rad.	10.6	10.5	10.5
60° Co^{60}	10.5	10.0	9.9
30° Co^{60}	10.5	10.3	10.0

precision of the measurements, which is of the order of ±1%. Certain trends in the data are already apparent and will be watched. For example, both groups of Li doped float-zone cells are degrading more rapidly than the crucible-grown Li doped cells. The most damaged type of all cells is the float-zone, low Li concentration. In the conventional boron-doped cells, the 60°C irradiation has produced slightly more damage than at 30°C.

The maximum exposure dose reported is 6.01×10^6 roentgens. This may be compared to a 1 MeV electron dose in two ways. First, one may compare the amount of gamma exposure with electron exposure on the basis of total absorbed dose (rads) per gram of silicon. This includes energy absorbed from both atomic displacement and ionization effects. On this basis the equivalent 1 MeV electron dose for 6.01×10^6 roentgens is about 1.8×10^{14} e/cm^2. However, one is not so much interested in ionization effects, as in displacement of silicon atoms. Using values[22] for the total number of displaced Si atoms per unit of incident flux of 10^{-2} for 1 MeV gamma photons and 4.6 for 1 MeV electrons, the equivalent 1 MeV electron dose corresponding to 6.01×10^6 roentgens is 2.6×10^{13} e/cm^2. One condition for this comparison is that the gamma irradiation is performed under conditions of electronic equilibrium. This is not the case in this solar cell irradiation, and further calculations and dosimetry will be performed to better define the received dose. The second calculation does give a figure which is in close agreement with previous 1 MeV electron data for n/p solar cells irradiated at 30°C.

2.3 Solar Cell Contacts

One aspect of solar cell technology that has received much attention is the process for making a durable, stable, low resistance contact. Many laboratories have reported the failure of solar cell contacts from environmental causes. A specific problem is that of huge increases in series resistance of solar cells exposed to high ambient humidity and temperature conditions. There is also the problem of the contact remaining ohmic at the low temperatures which will be encountered by outer planetary probes. Presently used contacts are mostly evaporated silver-titanium, with such added refinements as introducing platinum or palladium in an effort to reduce electrochemical corrosion. As an approach to overcoming the difficulties with the silver-titanium contact, the NRL solar cell contact program is investigating the formation of improved contacts through the use of ion implantation and sputtering techniques.

At 35 KeV bench accelerator was designed and constructed to produce ion beams for the implantation study. The n- and p-type dopants of current interest are phosphorus and boron. Other species, such as oxygen and nitrogen, are also planned for doping by implantation investigations (molecular nitrogen has a high bonding energy and is too large to enter silicon by diffusion). The noble gases are easily handled and are used for calibration purposes. The gas handling and ion source system is identical to that used on the NRL 5 MeV Van de Graaff. Therefore the techniques developed on the bench accelerator for handling dopants and metallic beams can also be used on the Van de Graaff accelerator.

A schematic of the 35 KeV accelerator is shown in Fig. 12. Gas is bled continuously into the quartz bottle and the pressure is controlled by a remote control valve. The gas pressure required depends upon the particular gas used and the desired beam intensity ($\sim 50\ \mu$ for BCl_3, $\sim 10\ \mu$ for the noble gases). The pressure in the accelerator and analyzing sections is such that the mean free path far exceeds the target ion source distance. The gas is ionized by a strong R. F. field and the external axial magnetic field increases the ionization probability. Positive ions are extracted from the induced plasma and accelerated through a series of electrostatic focusing lenses. The accelerating system can be adjusted to give an emerging ion beam energy from 5 to 35 KeV.

The ion beam that emerges from the accelerating system is well defined and slightly divergent. The focusing properties of the system are critically dependent upon the alignment of the beam into the analyzing magnetic field. Suitable slits and an electrostatic lens placed near the ion source are used to help define the beam. The mass range depends upon the energy of the ion beam; at 14 KeV the maximum mass of a resolved beam is 85 AMU.

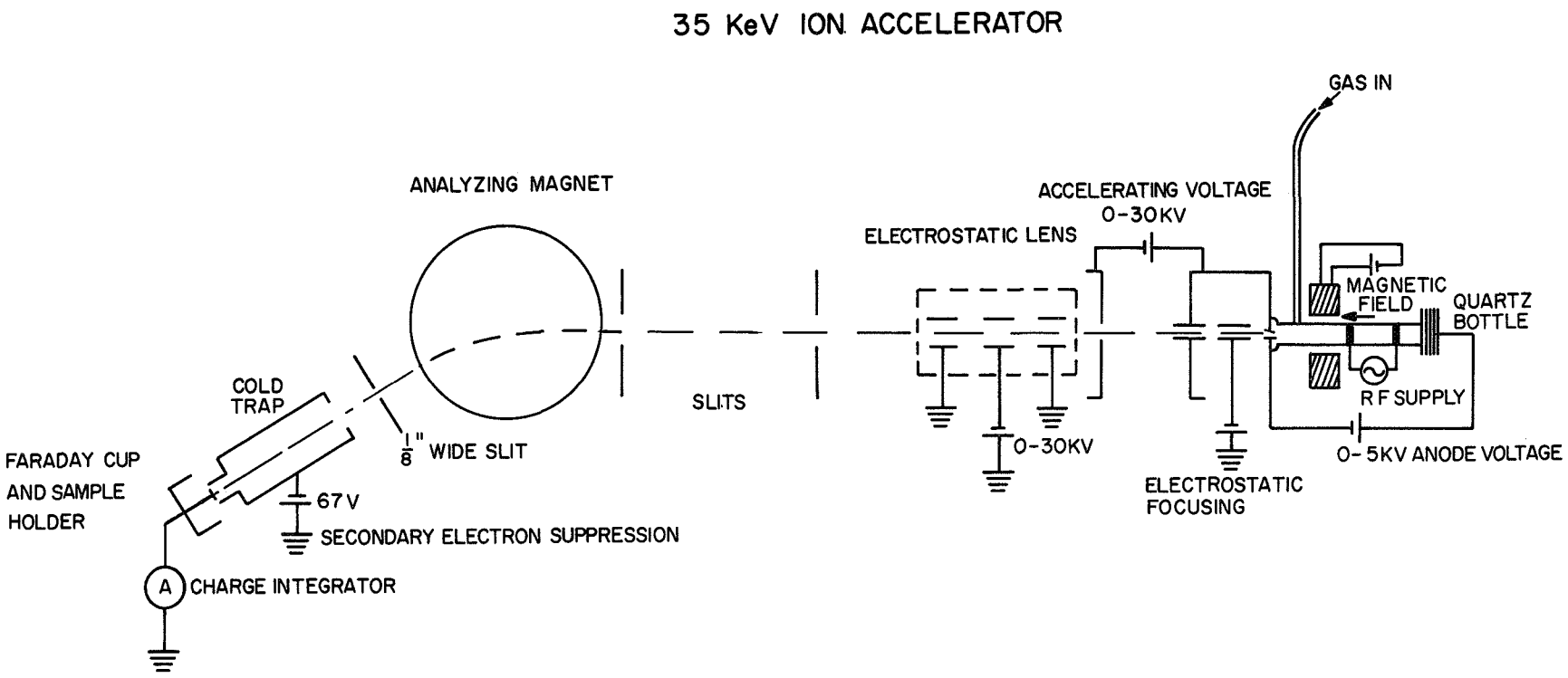

Figure 12 Schematic diagram of the 35 KeV ion accelerator.

The target holder, made of stainless steel and insulated from the system, serves as a charge collector in a Faraday cup arrangement. An analyzed beam of 2 cm^2 in area can be obtained with the above arrangement. An in-line LN_2 trap is negatively biased with respect to the target to suppress secondary electrons. A 20 KeV mass scan, using BCl_3 as the bleed-in gas, is shown in Fig. 13. The resolution (R) for such a scan is defined as $\frac{M}{\Delta M}$, where M is the mass number of the peak being considered and ΔM is the width of the peak measured at half the peak height. For a value of R = 2 M, an adjacent peak of equal height would contribute about 0.15% to the peak being measured. The resolution of the B^{11} signal is ~ 27, ensuring a pure beam. The surrounding mass peaks do not contribute to the B^{11} peak. Beams in the μA range have been obtained for the noble gases and B^{11} beams of ~ 50 nA have been obtained.

The Schottky diode was bombarded with boron as a possible means of reducing the capacitance by compensating for a heavy donor concentration near the diode surface. A 20 KeV boron beam with a current of 40 nA was delivered to targets 2 cm^2 in area. Preliminary studies showed that the capacitance of the diode could be reduced by 20% following a dose of 10^{17} boron ions/cm^2 at 20 KeV.

Beams of chromium and aluminum have been implanted in silicon at 60 KeV by the mass separator at the National Bureau of Standards (Mass Separator Group, N.B.S., Gaithersburg, Maryland). A target holder was constructed for the implants so samples could be heated up to 550°C while being bombarded. An Al beam of 10^{15} ions/cm^2 was implanted at 60 KeV on p-type, 1 ohm-cm silicon. Contacts were formed on top of the implanted region by sputtering on Au:In(1%).

The sputtered contacts thus formed exhibited non-ohmic behavior and were also sensitive to light. This is believed to be due to the presence of a p/n junction. The silicon may have become n-type near the surface as a result of the damage induced by the implantation process. After annealing at 400°C for two hours the contacts became ohmic and the light sensitivity disappeared. The implanted Al appears to produce an increased p-type surface and makes a better ohmic contact than the non-implanted silicon.

A metallic ion source (Hill and Nelson Sputtering Ion Source, sold by Radiation Dynamics, Inc., U.S.A.) has been ordered for use on the 35 KeV and 5 MeV accelerators. The ion-implantation and sputtering facilities have attracted the attention of other groups at NRL who are interested in contact formation or ion-doping of semiconductors and ferroelectrics. The facilities and capability will continue to be actively employed at NRL. However, the solar cell contact work is being suspended.

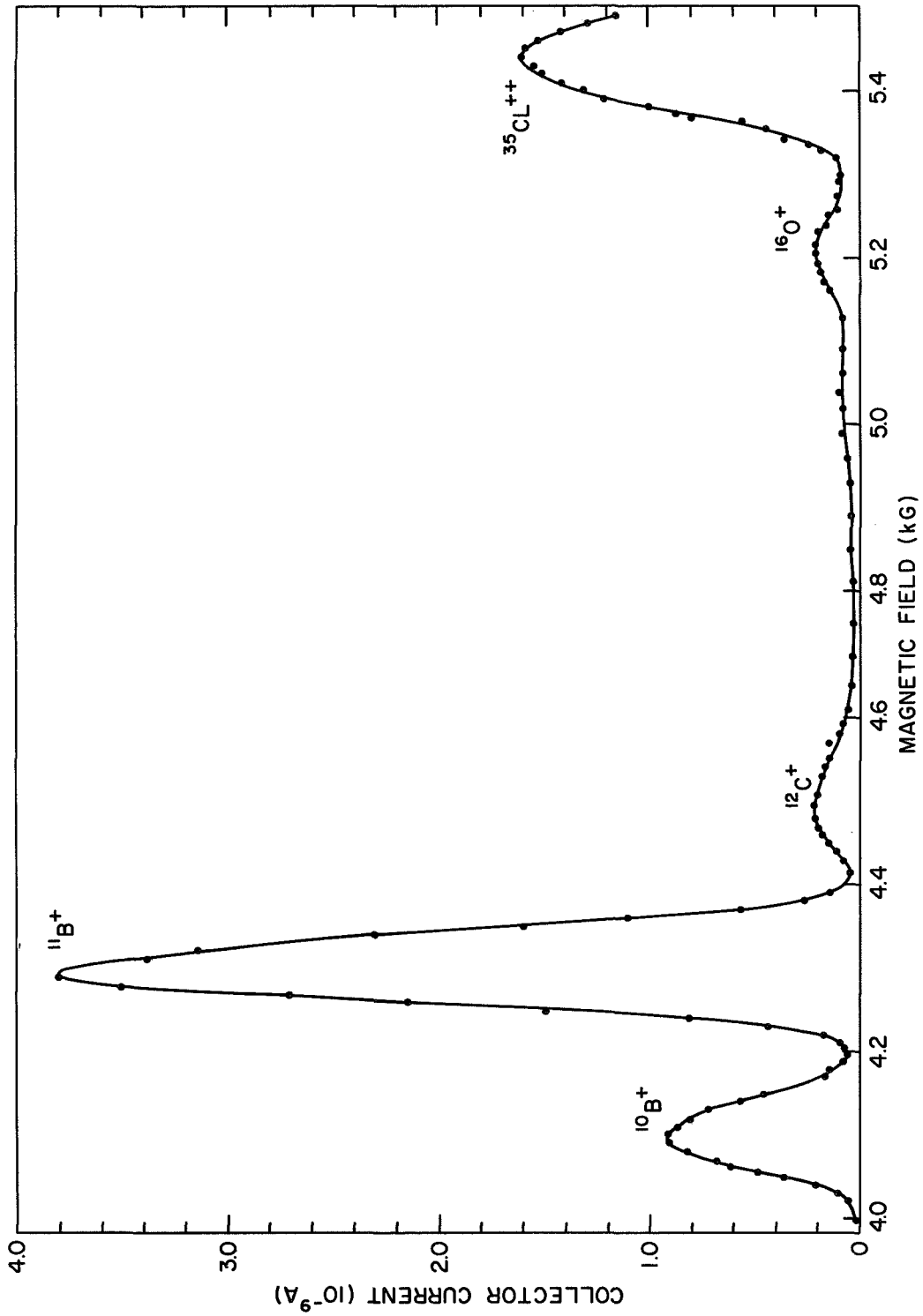

Figure 13 Mass scan obtained from the 35 KeV accelerator using BCl_3. The ion energy is 20 KeV.

2.4 Radiation Damage of Silicon Solar Cells at Low Temperatures

2.4.1. Introduction

A program has been initiated to study the effects of temperature on damage rate in electron-irradiated solar cells. While the temperature-dependence of the damage constant for gamma-irradiated p/n solar cells has been studied [23], there have been no corresponding results reported for n/p cells. The object of the current program is to determine the temperature dependence of the damage constant in p-type silicon.

The experiments of Gregory and Barnes [23] measured the irradiation-temperature dependence of carrier removal rates in n-type silicon and the short-circuit current degradation in p/n solar cells. While the carrier removal experiments essentially measure degradation in the majority carrier concentration, the solar cell is a minority carrier device and its efficiency is basically limited by minority carrier lifetime. The results of these experiments indicate that in irradiated n-type silicon, majority carrier removal rates are positively correlated with minority carrier lifetime degradation. That is, both types of damage are shown to increase as the irradiation temperature is increased.

The situation in p-type silicon is not clearly known. To date, no correlation between carrier removal and minority carrier lifetime degradation has been established. The importance of such a study for electron-irradiated n/p solar cells is evident. The consideration of solar cells for low-temperature environments such as the outer planetary satellites requires more knowledge and better understanding of wide-range temperature effects in solar cells.

2.4.2. Experimental

A few types of n/p solar cells have been irradiated and studied at low temperatures. The objectives of this preliminary phase of the investigation were (1) to determine the range of values for solar cell parameters at low temperature for some typical cells, (2) to compare the damage rate from 1 MeV electrons at low temperature and at room temperature, (3) and to evaluate the experimental techniques which were developed for mounting the samples and performing the irradiations and measurements.

The cells were mounted on a copper sample holder which was attached to a cold finger in a standard laboratory research dewar (Janis Model 6" -DT). The sample holder (see Fig. 14) was wound with a

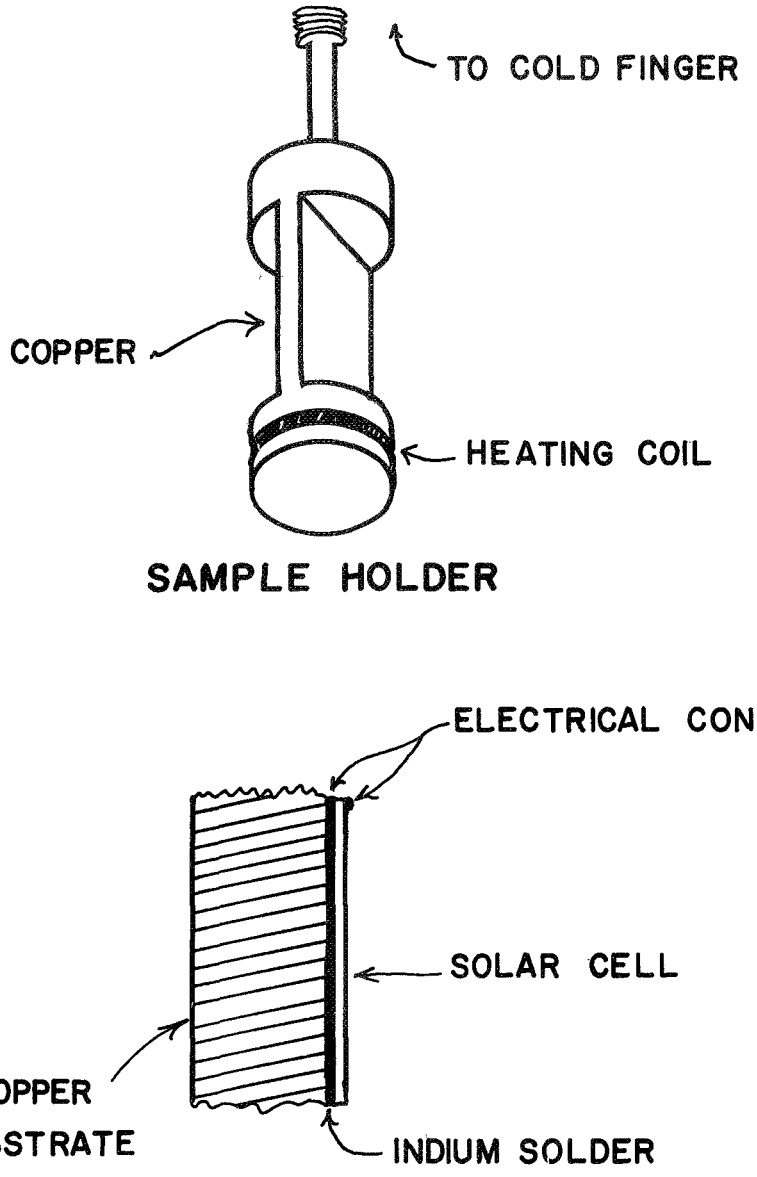

Figure 14 Sample holder and configuration for mounting solar cells. Four electrical leads were attached to the cell to eliminate voltage drops in the leads for the voltage part of the I-V measurements.

heating coil about the bottom of the holder. The connecting rod to the cold finger was small in diameter compared with the rest of the holder. Temperature control was achieved by balancing the conduction cooling through the rod with the heating provided by the coil; temperature was controlled to within ± 2°K by this technique. The cells were soldered to the sample holder with indium solder which "flows" at temperatures as low as liquid nitrogen temperature. Temperature was monitored throughout the irradiations and the I-V measurements by a thermocouple soldered to the main bus bar of the cell.

The cells were irradiated by 1 MeV electrons through a 3-mil aluminum window. The cells were kept dark in a vacuum at a temperature of 115°K. Following the irradiations the cells were maintained at this temperature or lower. I-V curves were then obtained at 115°K using a Spectrosun X-25 solar simulator. The cells were measured at various light intensities by interposing neutral density filters in the light path.

2.4.3. Results

Figures 15-19 give the I-V characteristics for three of the cells. These cells are 2 x 2 cm 10 ohm-cm n/p cells. Cells TI-109 and TI-121 were fabricated with a p^+ layer at the back surface to reduce the "Schottky barrier effect" whereas cell C-143 did not contain this layer. Nevertheless, the cells TI-109 and TI-121 at illumination levels of 70 mW/cm^2 and higher showed the "Schottky effect" developing under increasing electron radiation. At low light levels (~5mW/cm^2) it was not evident. Cell C-143 (see Fig. 19) exhibited this effect prior to the radiation. At low light levels and particularly at increased fluence this "tail" effect of the I-V curve near open-circuit conditions was enhanced.

Figure 20 gives a comparison between the degradation of efficiency for the cells irradiated and measured at 115°K and typical flight quality 10 ohm-cm n/p cells irradiated and measured at room temperature. The damage rate is higher for the cells irradiated at low temperatures than for those irradiated at room temperature. The large error bar on the 10^{14}e/cm^2 point for cell TI-121 is due to a large surge of beam current which occured during the irradiation. This current surge was detected by monitoring the irradiated solar cell current and the Van de Graaff instrumentation. The sample irradiation time was adjusted according to an estimate which necessarily involved some uncertainty in the time correction. Although this surge had never before been observed we have prepared for the measurement of similar beam current pulses by placing an integrating digital voltmeter in the system to monitor the beam current.

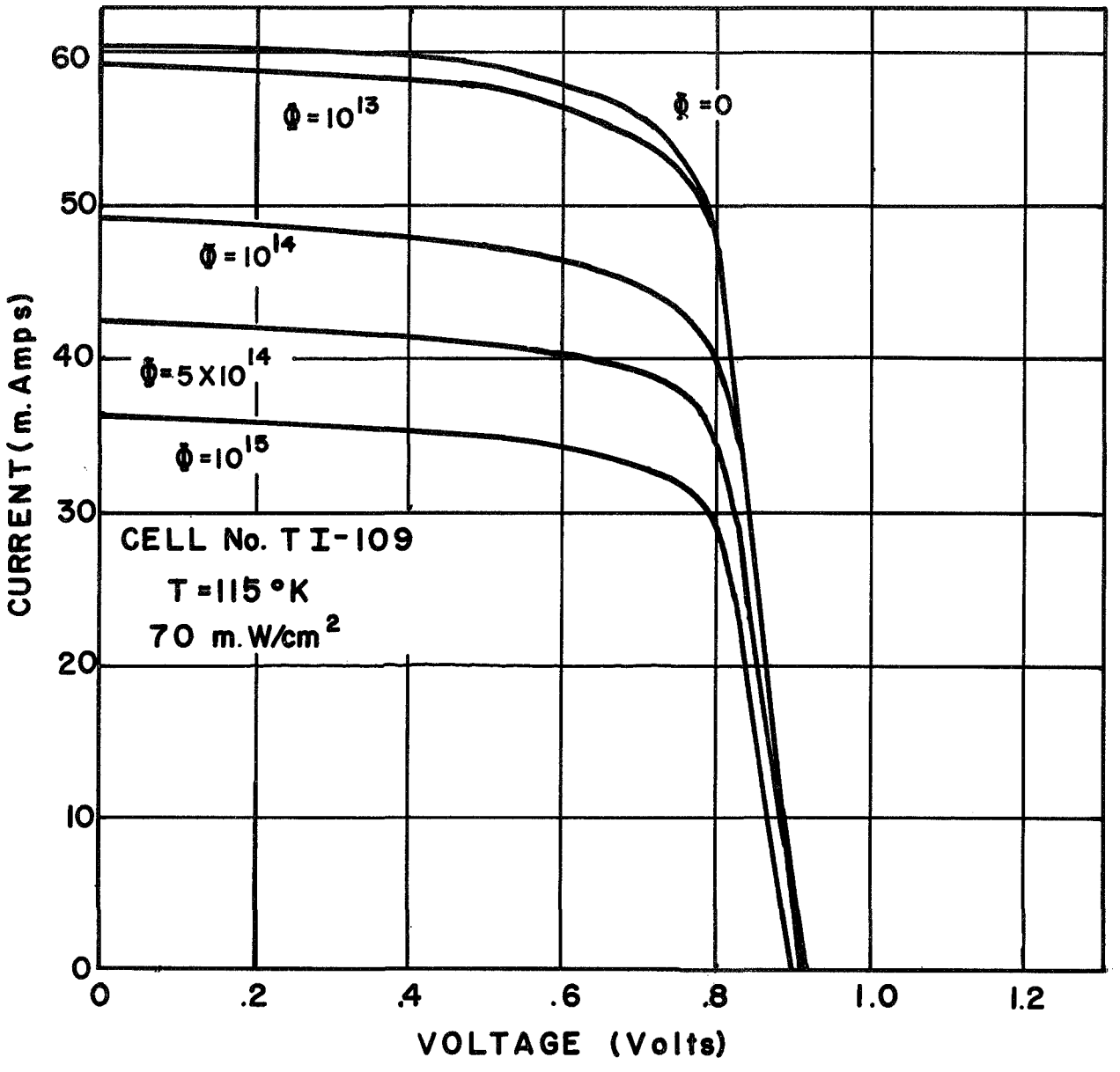

Figure 15 I-V characteristics of cell No. TI-109 as a function of 1 MeV electron fluence.

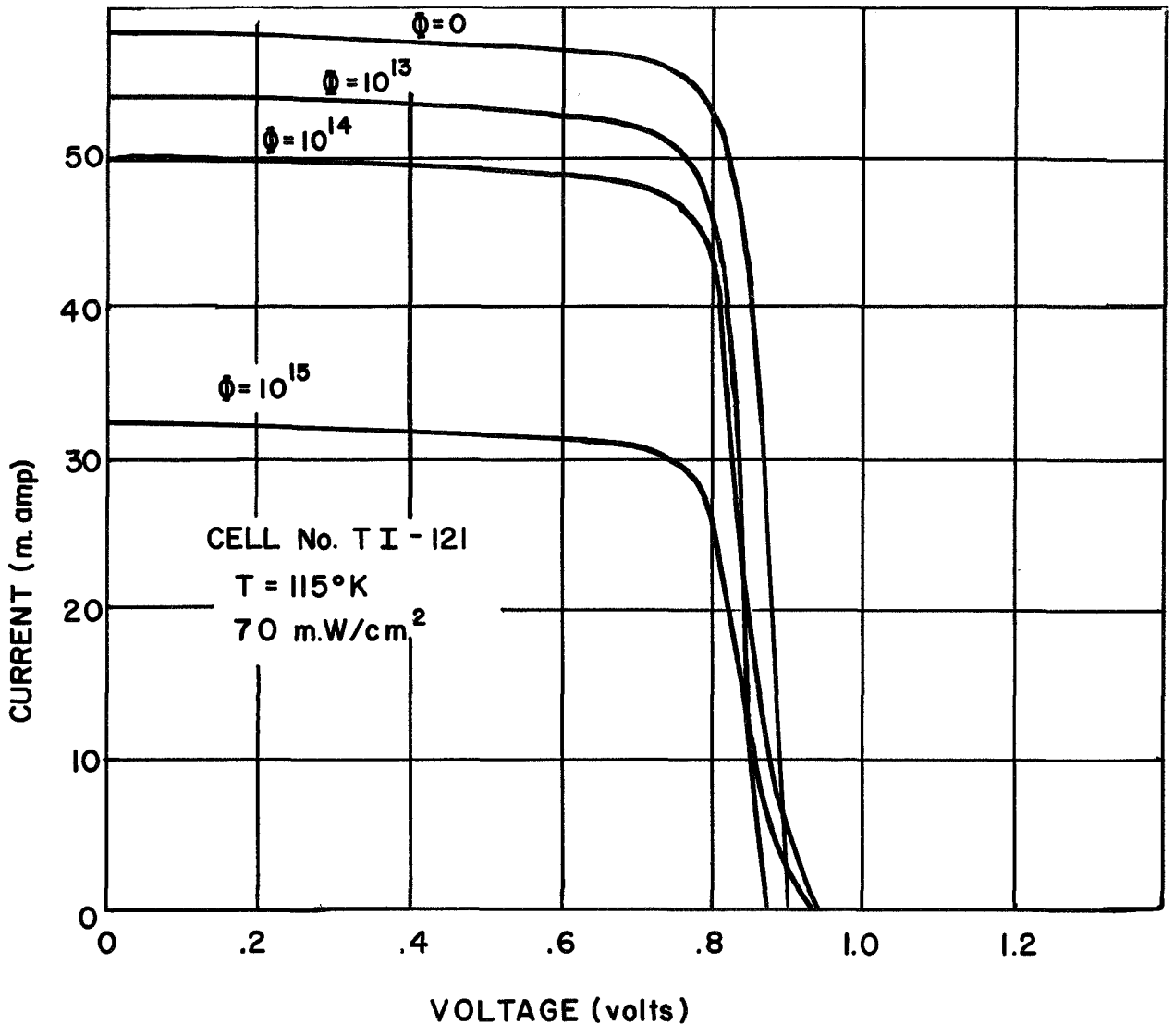

Figure 16 I-V characteristics of cell No. TI-121 as a function of 1 MeV electron fluence (e/cm^2). Note the curvature near open circuit at the higher fluences.

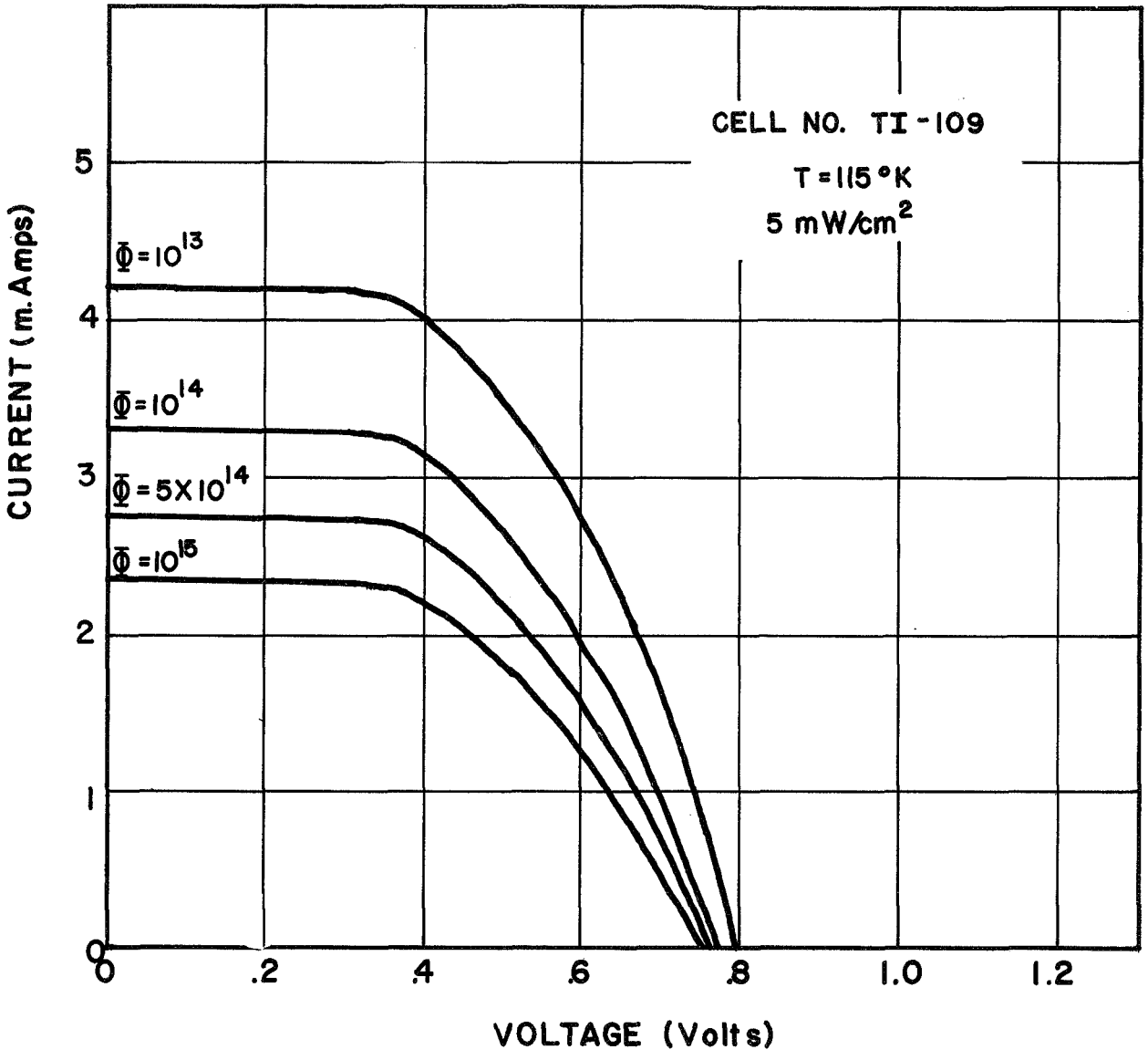

Figure 17 I-V characteristics for cell No. TI-109 as a function of 1 MeV electron fluence (e/cm^2).

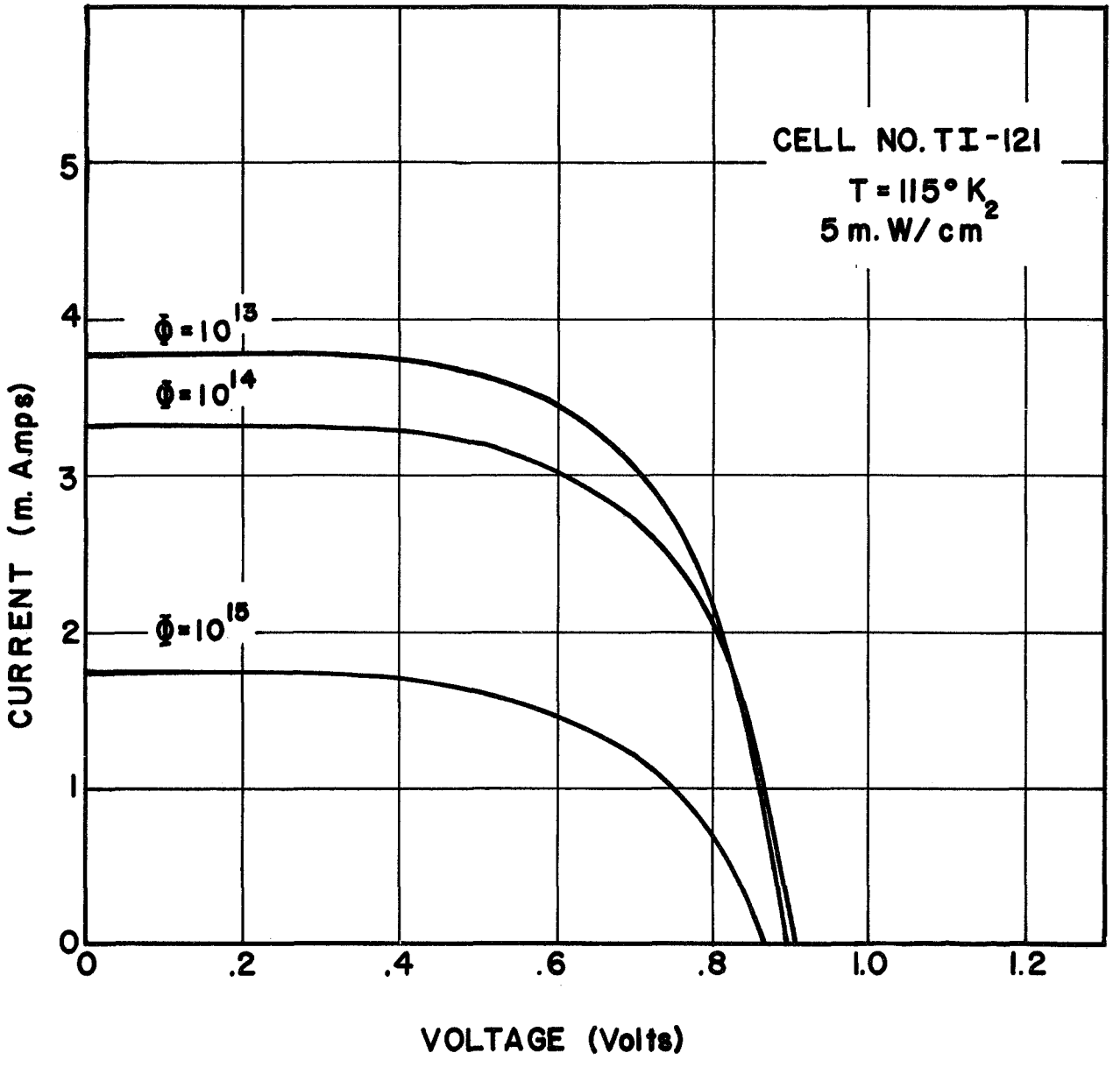

Figure 18 I-V characteristics for cell No. TI-121 as a function of 1 MeV electron fluence (e/cm^2). Note that for this illumination intensity (5 mW cm^2) as contrasted with that of 70 mW/cm^2, there is a lack of curvature near open circuit.

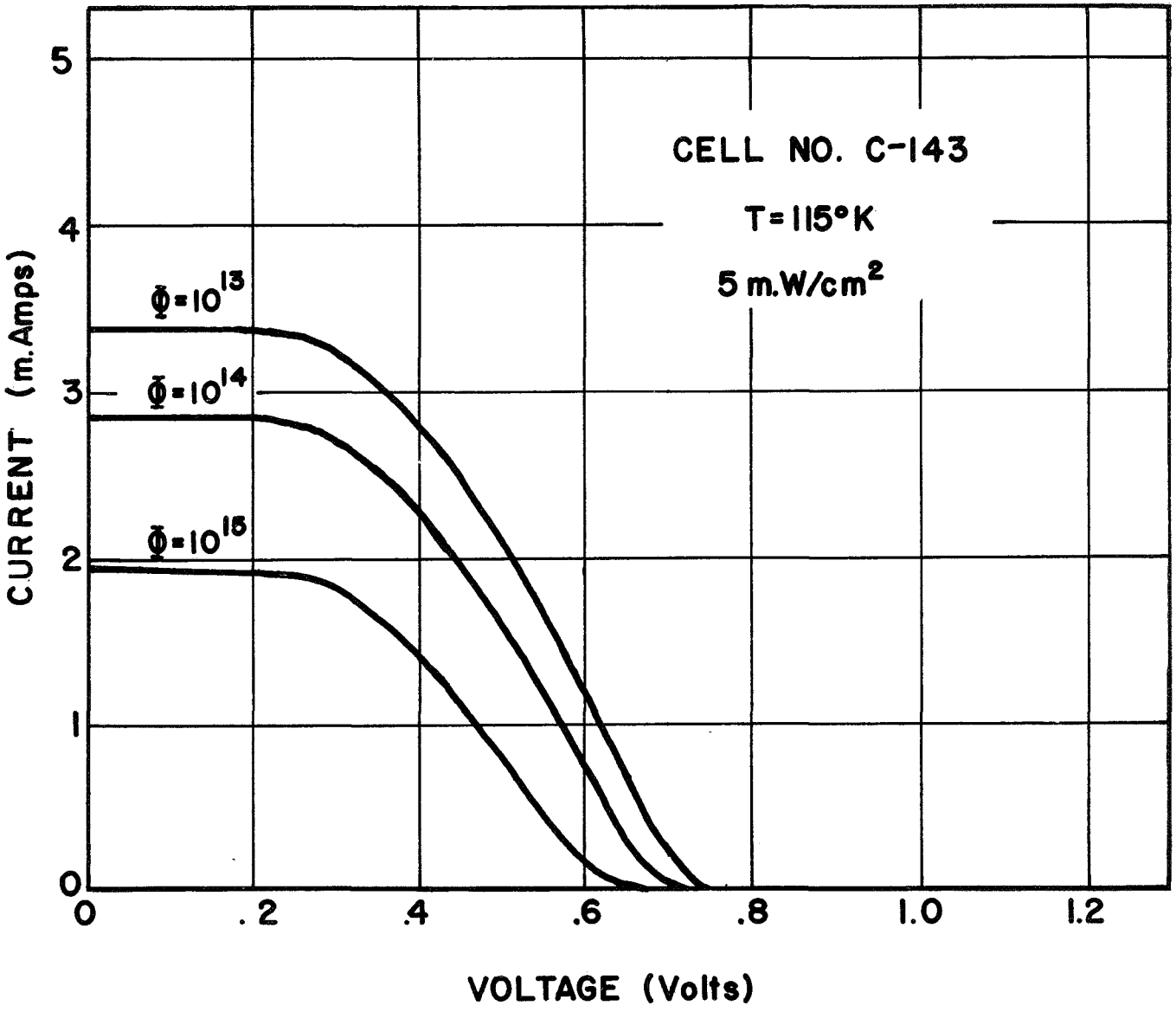

Figure 19 I-V characteristics for cell No. C-143 as a function of 1 MeV electron fluence (e/cm^2).

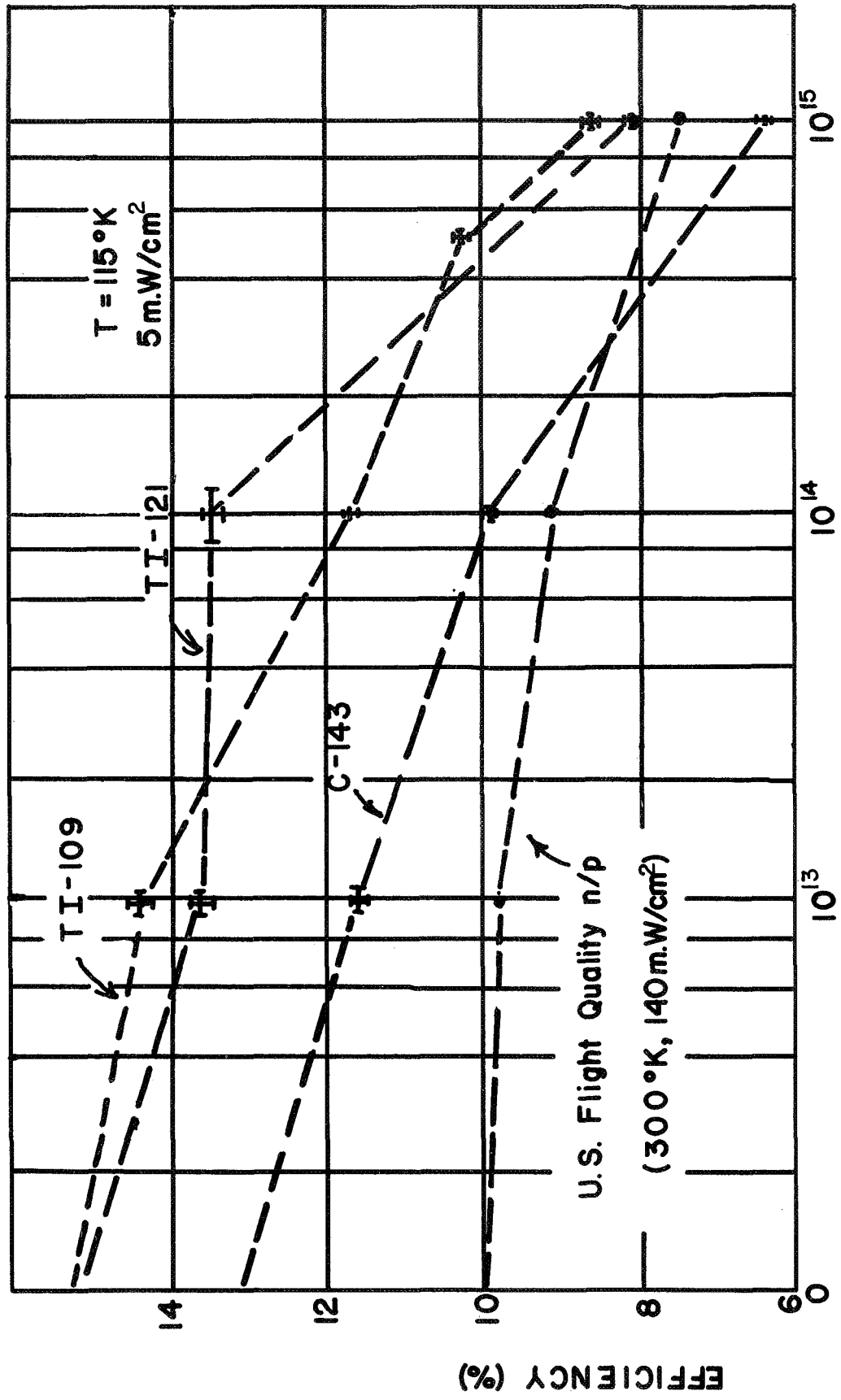

Figure 20 Conversion efficiency as a function of 1 MeV electron fluence. The cells which were irradiated and measured at 115°K are compared with those irradiated and measured at ~ 300°K.

The higher degradation rate at low temperatures is contrary to the carrier removal data of Novak [24]. He showed that the carrier removal rate in p-type silicon decreases with decreasing temperature until it is only 2/5 as large at 77°K as at 300°K. The corresponding change for n-type silicon is 1/20.

It is appropriate to comment on the statistical aspects of this study. The cells were irradiated one at a time due to space limitations in the dewar. A first consideration might suggest that an improvement would be made by irradiating several cells simultaneously. The gain in statistical confidence arising from a larger sample size is offset by the difficulties associated with maintaining uniformity in the electron beam and temperature control for a large group. The statistical confidence can be better established by performing a large number of irradiations using several cells of similar composition and exercising care in temperature control and dosimetry.

2.5 Analysis of Solar Cell I-V Characteristics

As an approach to analyzing solar cell I-V curves, a computer program has been written to fit experimental I-V data to the solar cell equation. The computer program has been adapted from a general least-squares program[8] which performs a least squares analysis for both nonlinear and linear functions. The maximum neighborhood method of Marquardt[25] is used. This method provides an optimum interpolation between the Taylor series method and the steepest-descent or gradient method. Convergence is assured at every interaction and speed of computation is maximized.

In addition, the program provides a statistical analysis of the fit. The statistical information provided is:

(1) the unbiased standard deviation of the function,

(2) the multiple correlation matrix of the parameters,

(3) the standard deviation of the parameters,

(4) the contour standard deviation,

(5) ellipsoidal estimates of the parameters,

(6) confidence limits on the value of the function.

Plotting subroutines are also provided which graph the experimental data, the best fit to this data, the 95% confidence limits on the data, and an error curve.

The solar cell equation is usually written in the form

$$I = I_L - I_o \left[\exp\left(\frac{V + IR_s}{V_o} \right) - 1 \right] \qquad (1)$$

where $V_o = AkT$

and A = a constant with value between 1 & 3

k = Boltzmann's constant (8.616×10^{-5} eV/^oK)

T = temperature (^oK)

I = load current

V = voltage across the cell

I_L = light generated current

I_o = reverse diode saturation current

R_s = effective series resistance of the cell

Equation (1) can be rewritten as

$$V = V_o \ell n\left(1 + \frac{I_L - 1}{I_o}\right) - IR_s \,. \tag{2}$$

The computer program as described above can be utilized to obtain a best fit of I-V data to Eq. (2), by treating I_L, I_o, V_o, and R_s as adjustable parameters. Since the short-circuit current, I_{sc}, and open-circuit voltage, V_{oc} are accurately measured, the number of adjustable parameters can be reduced from 4 to 2. The choice of the two parameters to be varied is arbitrary. For example, if I_L and I_o are chosen to be variable, Eq. (2) can be written as:

$$V = \frac{V_{oc}}{\ell n\left(1 + \frac{I_L}{I_o}\right)} \ell n\left(1 + \frac{I_L - 1}{I_o}\right) - \frac{I}{I_{sc}} \ell n \left(1 + \frac{I_L - I_{sc}}{I_o}\right). \tag{3}$$

The parameters A and R can be calculated from the values of I_o and I_L which give a best fit of the data to Eq. (3); that is,

$$A = \frac{V_{oc}}{kT \ \ell n \left(1 + \frac{I_L}{I_o}\right)} \tag{4}$$

and

$$R = \frac{AkT}{I_{sc}} \ell n \left(1 + \frac{I_L - I_{sc}}{I_o}\right) \tag{5}$$

Alternatively, R_s and V_o can be chosen to be variable and Eq. (2) becomes:

$$V = V_o \ell n[(1 - I/I_{sc}) \exp (V/V_o) + (I/I_{sc}) \exp (I_{sc}R_s/V_o)] - IR_s \quad (6)$$

The parameters A, I_o, and I_L can then be calculated from the best fit values of V_o and R_s:

$$A = V_o/kT, \quad (7)$$

$$I_o = I_{sc} / [\exp (V_{oc}/V_o) - \exp (I_{sc}R_s/V_o)] \quad (8)$$

and

$$I_L = I_o [\exp (V_{oc}/V_o) - 1] \quad (9)$$

While the solar cell equation as given above only approximates the behavior of real devices, it does fit experimental I-V data quite well. One limitation of this approximation is that the parameter A is not constant over the entire quadrant of the photovoltaic measurement. In theory, A = 1 for an ideal diode, while A = 2 when recombination in the space charge region limits the current. Higher values of A can be obtained if internal field emission takes place. Since it is not known precisely how A varies with voltage, A is usually treated as a constant. The deviation of experimental data from theory is most pronounced near the "knee" of the curve. Some of this deviation can possibly be explained by changes occuring in the parameter A as the solar cell is loaded for the I-V curve. Another limitation is the probability that the diode potential is distributed due to a sheet resistance in the surface layer of the cell. Thus, if the cell were considered to be comprised of N individual areas, the solar cell equation is written

$$I = I_L - \sum_{i=1}^{N} I_{o_i} \left\{ \exp [(V + IR_{s_i})/V_{o_j} - 1 \right\} \quad (10)$$

This equation contains 3N + 1 parameters and makes possible a closer fit to the data for N >1. However, as more parameters are used to fit the data, the more difficult it becomes to relate the equation to the measured physical parameters of the solar cell. Thus the close fit is obtained at the expense of a simply physical model or equivalent circuit of the solar cell.

The parametric study of the solar cell I-V curves has two applications. First, the statistical analysis gives an indication as to the applicability of this simple solar cell equation. Second, additional environmental factors such as temperature and irradiation fluence can be studied.

An example of the type of fit which can be obtained with the nonlinear least squares program is given in Figure 21. The overall fit can be seen to be quite good.

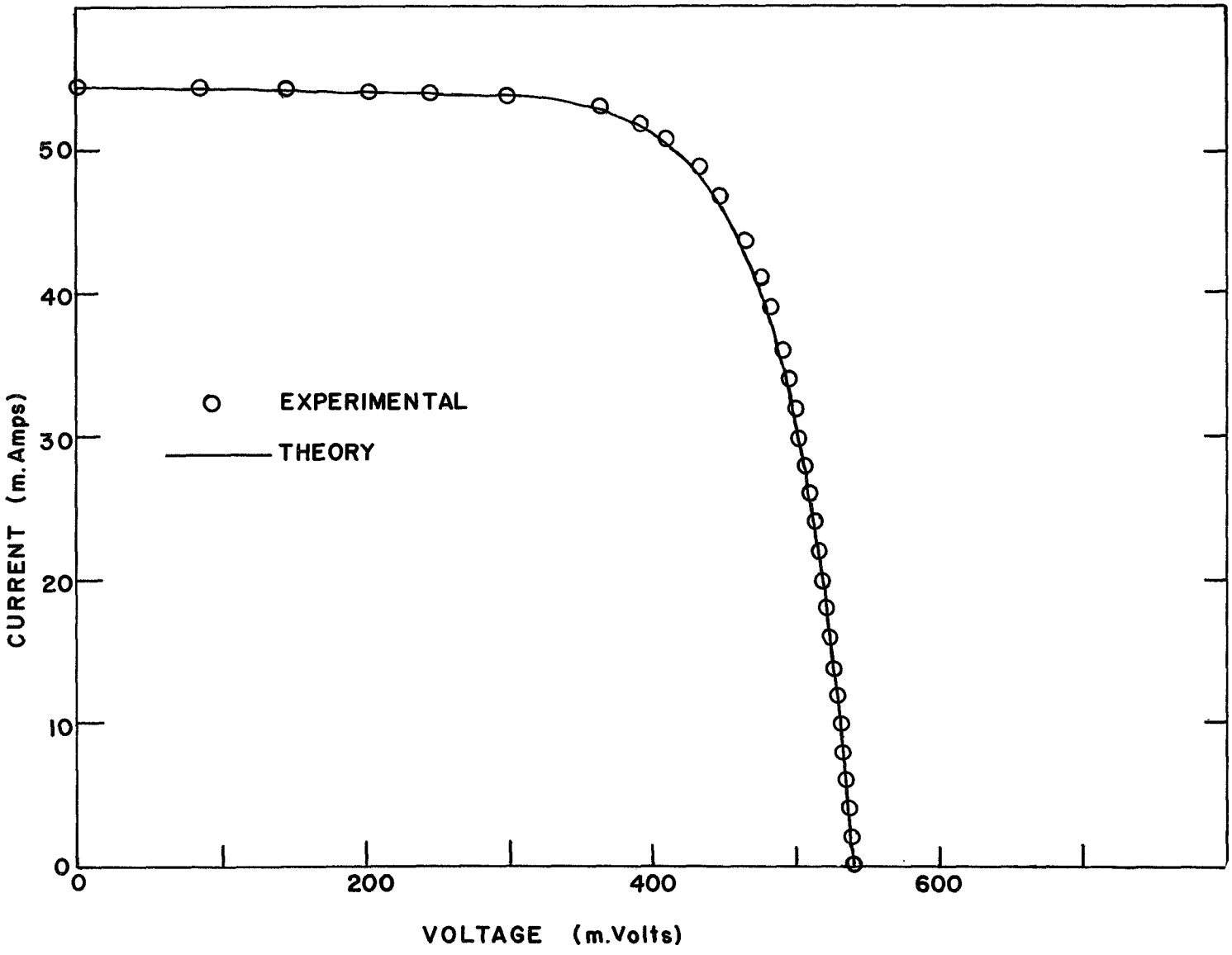

Figure 21 An example of the least-squares fit to the solar cell I-V characteristics using the lumped constant model (Eq. 6, Sec. 2.5). The fit is excellent except for the region of the "knee" of the curve.

2.6 Review of "Handbook of Space Environmental Effects on Solar Cell Power Systems"

2.6.1. Introduction

The Handbook of Space Environmental Effects on Solar Cell Power Systems released in January 1968 represents a revision, up-dating and expansion of an earlier handbook published in July 1963 as NASA Report SP-3007. The revised Handbook treats in more detail then its predecessor subjects such as the Theory of the Solar Cell, Radiation Damage to Solar Cells, the Space Radiation Environment, Satellite Test Data and Design Methods for Solar Cell Power Systems, Radiation Effects in Coverslides and Adhesives, and Radiation Effects on Power Conversion and Regulation Equipment. The last two topics were included as appendices in the earlier Handbook. New chapter headings include Instrumentation Techniques for Measuring Solar Cell Panels, Radiation Shielding of Solar Cells, and the Effect of Meteoroids on Solar Cell Arrays.

The present review was restricted to the Theory of the Solar Cell (Section II), Instrumentation Techniques for Measuring Solar Cell Parameters (Section III) and Radiation Damage to Solar Cells (Section IV). The first two sections were reviewed in great detail in the Semiannual Report for Solar Cell Research [26]. This review is summarized in the present report. Section IV is reviewed in detail. Some general recommendations on the format of the next edition of the Handbook are suggested, based on personal interviews with many workers in the solar cell community, both government and industrial.

2.6.2. Sections II and III

The Theory of the Silicon Solar Cell, Sec. II, is greatly improved onver a similar section in the first edition. It would be helpful to include additional references to more detailed discussion of p-n junction theory and photovoltaic effect. Also, the definitions of cell parameters and their interrelationships should be introduced earlier in the Handbook with greater clarity.

A serious deficiency in Section III is lack of data for unirradiated cells as a function of light source. Nowhere is there a comparison of cell parameters for a single group of cells measured under all the various light sources. The Handbook should be expected to reduce confusion which has arisen from the use of different light sources. A discussion of measurement accuracy and statistical sampling of representative solar cells from a group should be included.

It is also noted that no techniques are described for measuring the properties of solar cells as a function of temperature. Such measurements have assumed an increased importance in the light of planned explorations of the outer planets. The various types of variable temperature cell holders and dewars which have been used in such studies might be reviewed, as well as the manner of mounting the solar cells to the heat sink.

2.6.3. Review of Section IV

Section IV of the Handbook entitled "Radiation Damage to Solar Cells" is concerned with a subject of great importance to space power engineers, viz. the interaction of ionizing radiation trapped in the geomagnetic field with solar cells. This complex subject can be treated from many different aspects. For example, the engineer's primary interest may be in the degradation of the power output of a specific type of solar cell at a particular voltage under a definite fluence of 1 MeV electrons. Such information may only be of passing interest to a physicist attempting to identify the submicroscopic defect centers which influence the minority carrier lifetime in irradiated silicon. A Handbook should provide relevant information and guidance for the space power engineer as well as the radiation damage physicist. Such an attempt has been made in Section IV. The result is an incomplete and confused account of the radiation damage problem in solar cells. There is admittedly much useful information incorporated in the Handbook but it is presented in such a manner as to be unsatisfying to either the engineer or the physicist. One solution to the problem would be to prepare two completely independent treatments of the radiation damage problem - one should be concerned with the presentation of degradation data of the various solar cell parameters on commercially available cells over a comprehensive range of fluences, the other with a detailed description of the formation of various defect centers in silicon and their relation to the mechanism of radiation damage in solar cells.

Data presented in Section IV are helpful to the power engineer to indicate typical solar cell behavior following different irradiation conditions. But these would have been of far greater utility had the exact meaning conditions been stated in each case (light source) and had error bars indicated the typical spread of experimental values. A careful redrawing of many figures, e.g. 19, 20, 22, and 23, would also make the presentation more effective. The frequent utilization of the minority carrier diffusion length has doubtful value for the space power engineer. His primary interest is concerned with the degradation of the cells energy conversion capability in terms of power at a fixed voltage.

Degradation of the diffusion length has little significance for the engineer unless it can be related to power requirements. Additionally, very few laboratories have the capability to measure the diffusion length.

The principal criticism of the description of radiation damage mechanisms is the disconnected account of the damage problem in silicon with insufficient background. Thus there is a sudden introduction of A, E and J centers without any description of the silicon lattice or of the picture of defect centers by means of levels associated with the various centers in the forbidden gap.

A revised treatment of radiation damage mechanism for the physicist is recommended. Such a treatment should begin with a discussion of the silicon lattice and the band description of silicon. The established facts of the damage process should be presented first, leaving speculations and uncertain results for the latter part of the Section instead of interweaving the known with the unknown and uncertain as is done in the Handbook. Here too there should be a clear cut distinction made in the role of defect centers as they are related to minority carriers through recombination or to majority carriers through trapping. So far as solar cell damage is concerned, the former are of far greater significance. Considerable improvement of the present Section would also be achieved by an intensive literature search (1968 - to the present) of Journal articles.

2.6.4. Recommendations

Personal discussions and interviews have been held with government and industrial solar cell engineers and scientists. The majority opinion held that a solar cell handbook could be very useful. Some suggested uses of the Handbook are (1) to provide an orientation source source for new photovoltaic specialists, (2) for use in a technical course in solar cell theory and solar panel design, (3) for day to day use by systems designers for rough calculations (where the precision which requires computer analysis would not be demanded).

The present Handbook received much favorable comment as representing an improvement over the first edition. One of the frequent unfavorable criticisms referred to the method of presenting Section IV on Radiation Damage. The specific criticism was directed toward the use of minority carrier diffusion length as the parameter to define degree of radiation damage. This criticism came primarily from array designers who apparently almost universally prefer the concent of equivalent 1 MeV electron damage in solar cells to that of diffusion length for calculating radiation spectrum effects on solar cells. The following specific recommendations are made, based on the personal survey of users.

(1) Restructure the Handbook format into three independent, self-coherent and self-sufficient sections: one treating the physics of solar cell operation and radiation effects from a band picture and energy level considerations, a second section describing measuring techniques, instrumentation, and design of experiments, and a third part containing data and procedure for designing solar arrays, with illustrative examples.

(2) Use of loose leaf binding as in the Handbook on Transient-Radiation Effects on Electronics [22], so that only sections requiring up-dating will be revised in the future. Also new tables of data, e.g. solar cell characteristics as a function of illumination and temperature, changes in the radiation environment, etc., can be inserted as they become available.

(3) Obtain contributions to the writing of the Handbook from many authors who are acknowledged experts in various specialties. This approach would require a central editorial group whose responsibility would be to determine the author's whose services are desirable. This editorial group of course must also be expert in some aspects of photovoltaics.

3.0 CONCLUSIONS

From the cryogenic Hall measurements made in float zone silicon doped with lithium, it was found that irradiation at low temperature was necessary in order to separate the recovery from the damage process. Measurements made on lightly doped material indicated the presence of the LiO donor with a thermal activation energy of approximately 0.0375 eV. A deep level about 0.15 eV below the conduction band was observed subsequent to irradiation and annealing. The nature of this center is not presently known.

The low flux gamma irradiation of lithium diffused solar cells disclosed the presence of a continuous damage process in some types of lithium-silicon solar cells over long periods of irradiation. This appears more predominantly in crucible grown and Lopex silicon than in float-zone. The first experiment which was continued from the NASA-GSFC study encompassed too many variables with insufficient sample size. The redesigned experiment is yielding data with a precision of ± 1% in maximum efficiency.

The ion implantation work progressed to the point of successfully producing a controlled boron beam which was used to implant boron ions in a Schottky barrier diode. This resulted in a change in capacity of the diode which verified the implantation of boron into the surface. The boron beam was variable in energy from 5 to 35 KeV. Other ions, such as nitrogen and phosphorus, can be implanted in a similar manner.

Measurement of solar cell efficiency over the range of room temperature down to liquid nitrogen temperature revealed that in some cells the efficiency improves up to 16% at the low temperatures. These data show that solar cell contacts may become a problem in some silicon cells (e.g. 1 ohm-cm p/n and 10 ohm-cm n/p) at low temperatures. Electron-irradiation of n/p solar cells at temperatures of 115^{o}K indicate a damage rate which is greater (perhaps several-fold) than the damage rate at room temperature. These preliminary results on a very few samples indicate important areas for further investigation.

A general least-squares program was adapted for curve-fitting of the diode equation to experimental I-V curves. The four adjustable-parameter fitting process provides a close approximation of the diode equation to most solar cell I-V curves. This analysis is useful for studying solar cell parameters as a function of temperature and radiation fluence.

A review of Sections II, III, and IV in the "Handbook of Space Environmental Effects in Solar Cell Power Systems" was made. In general, these portions of the Handbook are greatly improved over those in the first edition in clarity and inclusiveness.

It is suggested that the introduction of solar cell parameter definitions together with their functional dependencies would be valuable near the beginning of the Handbook. There is a need for a more detailed explanation of temperature effects on solar cell properties and a description of experimental techniques required for measurement of temperature effects. The subject of radiation damage in solar cells needs to be presented in two ways: one which will discuss the physical interaction of particle radiation with the silicon crystal on a submicroscopic basis, and treat the subjects of defect production, lifetime degradation, and annealing kinetics in a satisfying manner for solid state physicists; the other treatment of this topic would give tables, charts, and nomographs of the radiation damage characteristics of specific type of cells as a function of fluence, temperature, and illumination in such detail as to enable an engineer to design a solar array for specifically known environmental conditions. This diversity of user's requirements suggest a restructuring of the Handbook format into three independent, self-sufficient sections: one concerned with the basic physics of solar cell operation and radiation effects, a second describing measuring techniques for solar cell properties, instrumentation, and design of experiments, and a third section illustrating design procedures for solar arrays.

4.0 RECOMMENDATIONS

The Hall coefficient measurements have proven to be extremely useful in analyzing the behavior of lithium in irradiated silicon. This work will continue using silicon with low lithium concentrations, since the lithium interactions may become increasingly complicated as the lithium concentration is increased. The relationship between the observed deep level and the presence of lithium should be established. Additional measurements of defect concentrations as a function of 300°K annealing will be carried out.

Efforts will be made to improve thermometry and data collection efficiency. The Hall sample homogeneity is being measured and improvements may be made if possible.

The low flux Co^{60} gamma experiment will be continued with data-taking at useful intervals. The actual dose received by the cells will be measured by dosimetry methods, probably using solid-state materials. Correlation of Co^{60} damage rate in solar cells will be made with 1 MeV electron damage in similar samples.

Specific work on solar cell contacts will be terminated at this time. The ion implantation work will continue to be carried out at NRL under other support. Future developments in this area may have application to solar cell technology.

Low temperature electron irradiation of several resistivities of n/p solar cells, 1 x 2 cm, solderless contacts, will be carried out. These cells are on hand in sufficient quantities to give statistically important data. In addition to I-V characteristics, spectral response measurements and ultimately diffusion length studies will be made to determine damage constant values. These cells will be compared with cells irradiated at room temperature and measured at liquid nitrogen temperature.

The computer curve-fitting technique will be applied for data analysis as appropriate. It is conceivable that low temperature irradiation data may not be well-represented by the four adjustable-parameter equation. If so, additional consideration will be given to modifying the diode equation.

It is considered that any additional detailed review of the Handbook of Space Environmental Effects on Solar Cell Power Systems is not necessary at this time, in view of the recommendations for massive restructuring of a future edition as suggested in Section 2.6.4.

5.0 ACKNOWLEDGEMENTS

Thanks are due P. Berman of JPL, P. Iles of Centralab, and R. Debs of NASA-Ames for providing solar cells for radiation studies.

6.0 NEW TECHNOLOGY

1. Technique for mounting a silicon solar cell to dewar cold finger for photovoltaic measurements at temperatures from 300°K to 80°K.

Originated by R. J. Lambert.

Described in Semiannual Report for Solar Cell Research, p. 24, 15 April 1969.

REFERENCES

(1) J. W. Corbett, in Solid State Physics, F. Seitz and D. Turnbull, Eds. (Academic Press, Inc., New York, 1966), Supplement 7.

(2) I. V. Smirnova, V. A. Chapnin, and V. S. Vavilov, Soviet Phys. - Solid State 4, 2469 (1963).

(3) E. Sonder and L. C. Templeton, J. Appl. Phys. 34, 3295 (1963).

(4) G. J. Brucker, Phys. Rev. 183, 712 (1969).

(5) A. C. Beer, in Solid State Physics, F. Seitz and D. Turnbull, Eds. (Academic Press, Inc., New York, 1963), Supplement 4.

(6) D. Long and J. Myers, Phys. Rev. 115, 1107 (1959).

(7) J. Messier and J. Merlo Flores, J. Phys. Chem. Solids 24, 1539 (1963).

(8) A program using the method of least squares was obtained from the University of Maryland for this purpose. W. G. Daniels, Tech. Rept. 579, 1966 (unpublished). Subroutines were written here for the various models tried.

(9) E. L. Ralph, G. S. Goodelle, P. Payne, "Investigations of Lithium Doped Hardened Solar Cells", Quarterly Technical Report, Contract AF 33615-67-C-1458, Heliotek, 1 August 1967.

(10) J. P. Maita, J. Phys. Chem. Solids 4, 68 (1958).

(11) C. J. Ammerlaan and W. E. Vander Vliet, Phys. Rev. Letters 23, 470 (1969).

(12) H. J. Stein and R. Gereth, J. Appl. Phys. 39, 2890 (1968).

(13) J. D. Carter, Jr., and R. G. Downing, "Radiation Damage in Lithium Doped Silicon and Silicon Solar Cells" Semiannual Progress Report, Contract NAS 5-10322, TRW Systems, 28 August 1966.

(14) H. J. Stein and F. L. Vook, Phys. Rev. 163, 790 (1967).

(15) R. L. Aggarwal, P. Fisher, V. Mourzine, and A. F. Ramdas, Phys. Rev. 138, A882 (1965).

(16) R. L. Agarwal and A.K. Ramdas, Phys. Rev. 137 A602 (1965).

(17) W. Kohn, in Solid State Physics, F. Seitz and D. Turnbull, Eds. (Academic Press, Inc., New York, 1957), Vol. 5.

(18) E.M. Pell, J. Appl. Phys. 32, 1048 (1961).

(19) W. Kaiser and P. Keck, Phys. Rev. 101, 1264 (1956).

(20) R.A. Schmidt, "Degradation of Solar Cells", Final Report, Task 713-2220, Electro-Mechanical Research, Inc., 31 August 1968.

(21) P.H. Fang, "Gamma Irradiation of Lithium Silicon Solar Cells", Conf. Record of the Seventh Photovoltaic Specialists Conference, p. 113, 19-21 November 1968.

(22) Transient-Radiation Effects on Electronics Handbook, DASA 1420, edited by R.K. Thatcher, Battelle Memorial Institute, August 1967.

(23) B.L. Gregory and C.E. Barnes in Radiation Effects in Semiconductors, Plenum Press, New York, 1968, pg. 124, (F.L. Vook, Ed.)

(24) R. L. Novak, Dissertation, University of Pennsylvania, (1964).

(25) D.W. Marquardt, J. Soc. Indust. Appl. Math. 11, 431 (1963).

(26) "Solar Cell Research" Semiannual Report, Naval Research Laboratory, DPR WO-8056, 16 April 1969.

APPENDIX A

Two Impurity Model

The interaction of an electron with a donor impurity can be written as a chemical reaction

$$D^{o} \rightarrow D^{+} + \eta \tag{A1}$$

The law of mass action can be written

$$\frac{D^{+}\eta}{D^{o}} = Q \tag{A2}$$

From Fermi statistics:

$$D^{o} = \frac{D}{1 + g^{-1} e^{(d-f)/kT}} \tag{A3}$$

for non degenerate statistics in the conduction band

$$\eta \simeq N_{c} e^{(f-c)/kT} \tag{A4}$$

The equilibrium constant is shown to be

$$Q = \frac{N_{c}}{g} e^{(d-c)/kT} \tag{A5}$$

by using A2 through A4 and the fact

$$D = D^{+} + D^{o} \tag{A6}$$

The presence of the acceptors, which are all negatively charged in n-type material, is evident through the requirement of charge neutrality:

$$\eta + A = D^{+} \tag{A7}$$

A2 can be rewritten as

$$\frac{(\eta + A)\,\eta}{D - (\eta + A)} = \frac{N_c}{g}\, e^{(d-c)/kT} \qquad (A8)$$

A best fit of this form to the data, $[\eta, T]$ is obtained by varying the four parameters:

g = ground state degeneracy of the donor

D = donor concentration

d = donor activation energy

A = acceptor concentration

Equation (A8) can be understood in terms of approximations that are valid for certain temperature regions and certain doping concentrations.

High temperatures and all dopant concentrations

$$\eta \sim D - A \ , \qquad (A9)$$

Low temperature and comparable donor and acceptor concentrations

$$\eta \sim \frac{D-A}{A}\ \frac{N_c}{g}\ e^{\frac{d-c}{kT}} \ ; \quad \eta \ll D,\ D > A \qquad (A10)$$

Low temperature and very small acceptor concentration

$$\eta \sim \frac{DN_c}{g}\ e^{\frac{d-c}{2kT}} \ ; \quad \eta \sim A,\ A \ll D \qquad (A11)$$

Very low temperature and very small acceptor concentration

$$\eta \sim \frac{D-A}{A}\ \frac{N_c}{g}\ e^{\frac{d-c}{kT}} \ ; \quad \eta \ll A,\ A \ll D \qquad (A12)$$

These approximations are included here to show the dependence of carrier concentration upon temperature. In this work a program also was used which varied the four parameter, A, D, d, and g in the exact equation (A8) until a least squares best fit was obtained.[8]

A = acceptor concentration

D = total donor concentration

$[D^{o}, D+]$ = concentrations of neutral and positively charged donors respectively

η = carrier concentration (electron)

Q = equilibrium constant

c = energy of conduction band edge measured positvely upward from valence band

f = Fermi energy measured upwards from valence band

d = donor energy measured upward from valence band

g = degeneracy of donor ground state

k = Boltzmann constant

T = absolute temperature

N_c = conduction band effective density of states